the SILK ROAD PROJECT at NAOC

丝绸之路 计划

ZENTRUM FÜR ASTRONOMIE

ARI ITA LSW Univ. Heidelberg

Deutsche Forschungsgemeinschaft DFG

# Dynamics of nuclear and globular clusters, neutron stars, black holes, gravitational waves


**Rainer Spurzem, and Silk Road Team**

**Kavli Institute for Astronomy and Astrophysics (KIAA), Peking University**

**National Astronomical Observatories (NAOC), Univ. of Chinese Academy of Sciences**

**Astronomisches Rechen-Inst., ZAH, Univ. of Heidelberg, Germany**


**Dec. 3, 2024**

**ITP Frankfurt**

***Picture:***

**Xi Shuang Banna, Yunnan, SW China (R.Sp.)**


spurzem@ari.uni-heidelberg.de

spurzem@nao.cas.cn

https://astro-silkroad.eu


VolkswagenStiftung

**1) Introduction, History, Theory**

2) Star Cluster Dynamics with
Black Holes and Gravitational Waves

3) Nuclear Star Clusters

4) People, Code(s) and Hardware

5) Summary and References

# University of Heidelberg: ARI/ZAH, connected with IMPRS
# Every year graduate school application deadline (November)

https://zah.uni-heidelberg.de/institutes

https://www.imprs-hd.mpg.de/

The **Zentrum für Astronomie der Universität Heidelberg (ZAH)** was established in 2005 by joining the Astronomisches Rechen-Institut (ARI), the Landessternwarte Königstuhl (LSW) and the Institut für Theoretische Astrophysik (ITA).

## Astronomisches Rechen-Institut (ARI)

Mönchhofstr. 12-14
69120 Heidelberg
Tel: 06221 54 1801

## Institut für Theoretische Astrophysik (ITA)

Albert-Ueberle-Str. 2 and
Philosophenweg 12
69120 Heidelberg

## Landessternwarte Königstuhl (LSW)

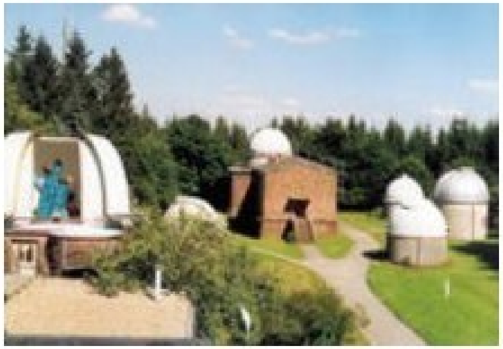

Königstuhl 12
69117 Heidelberg
Tel.: 06221 54 1700

Self Service | Contact | Sitemap

IMPRS-HD

International Max Planck Research School for Astronomy & Cosmic Physics at the University of Heidelberg

ABOUT THE SCHOOL | APPLICATION | RESEARCH | ACADEMICS | PEOPLE | PRACTICAL INFORMATION | SUMMER SCHOOL 2022 | Search

IMPRS FELLOWS | MISCELLANEOUS | IMPRS CALENDAR | COVID-19

Astronomisches Rechen-Institut (ARI) at U.f Heidelberg;

**founded May 10, 1700**

Siemens 2002 Computer in 1964 At ARI

# Kavli Institute for Astronomy and Astrophysics, Peking Univ..


*Total ~25 postdocs; 2/3 are non-Chinese.*

**Founded 2008**

**Regular Openings:**

**Postdoc**
**Faculty**
**Visitors**
**(see AAS Job Reg, search KIAA)**

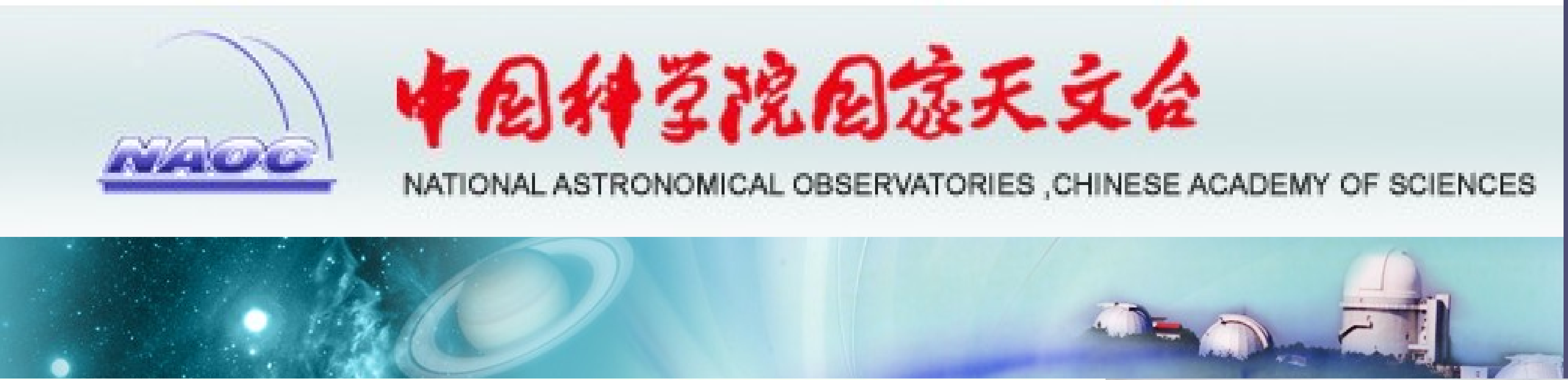


# NAOC/ CAS


**Silk Road Project =**

**Computational Science Project...**

Top: NAOC Headquarter Beijing

Bottom: LAMOST Site

# Star Clusters: Modelling the Dynamics

**(coupling of scales)**

$$\vec{a}_0 = \sum_j G m_j \frac{\vec{R}_j}{R_j^3} \quad ; \quad \dot{\vec{a}}_0 = \sum_j G m_j \left[ \frac{\vec{V}_j}{R_j^3} - \frac{3(\vec{V}_j \cdot \vec{R}_j)\vec{R}_j}{R_j^5} \right]$$

- $N = \infty$

negative specific Heat

gravothermal Collapse

gravothermal Oscillations

- $N = 3$ $(N = 2, \ldots, \approx 100)$

History

Exponential Instability

Chaos and Resonance

Regularisation

- $N = 10^6$ $(N = 10^4, 10^5)$

Post-Kollaps-Evolution

Binaries

Globular Clusters

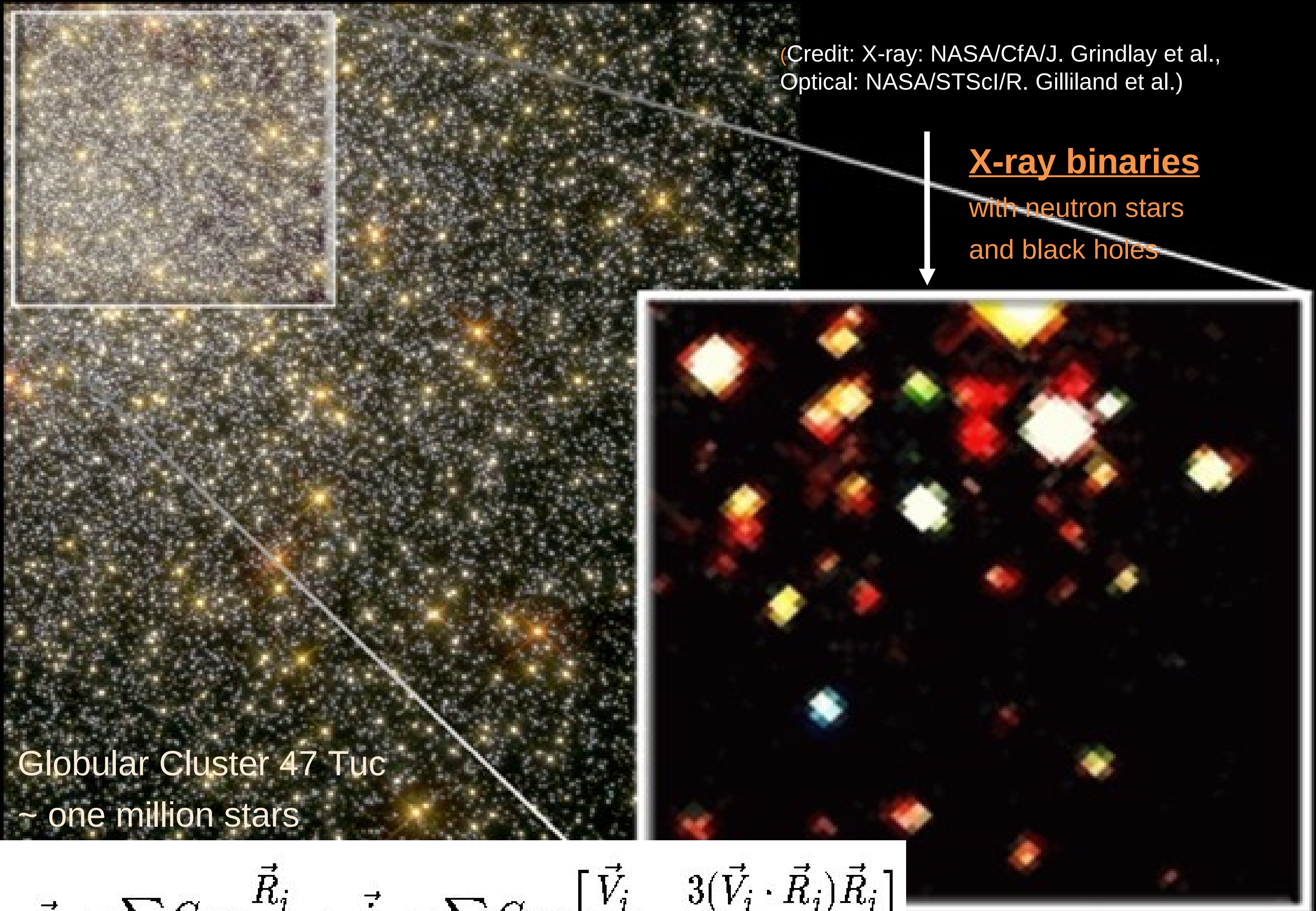


$$\vec{a}_0 = \sum_j G m_j \frac{\vec{R}_j}{R_j^3} \quad ; \quad \dot{\vec{a}}_0 = \sum_j G m_j \left[ \frac{\vec{V}_j}{R_j^3} - \frac{3(\vec{V}_j \cdot \vec{R}_j)\vec{R}_j}{R_j^5} \right]$$

# Star Clusters: Modelling the Dynamics

## (Manage deterministic chaos)

Chaos in 3-body Encounters

Starlab Simulation (S.L.W. McMillan)

http://www.physics.drexel.edu/~steve/

**Gravothermal Oscillations - Attractor in Phase Space**

Spurzem 1994, Giersz & Spurzem 1994

Amaro-Seoane, Freitag & Sp. 2004

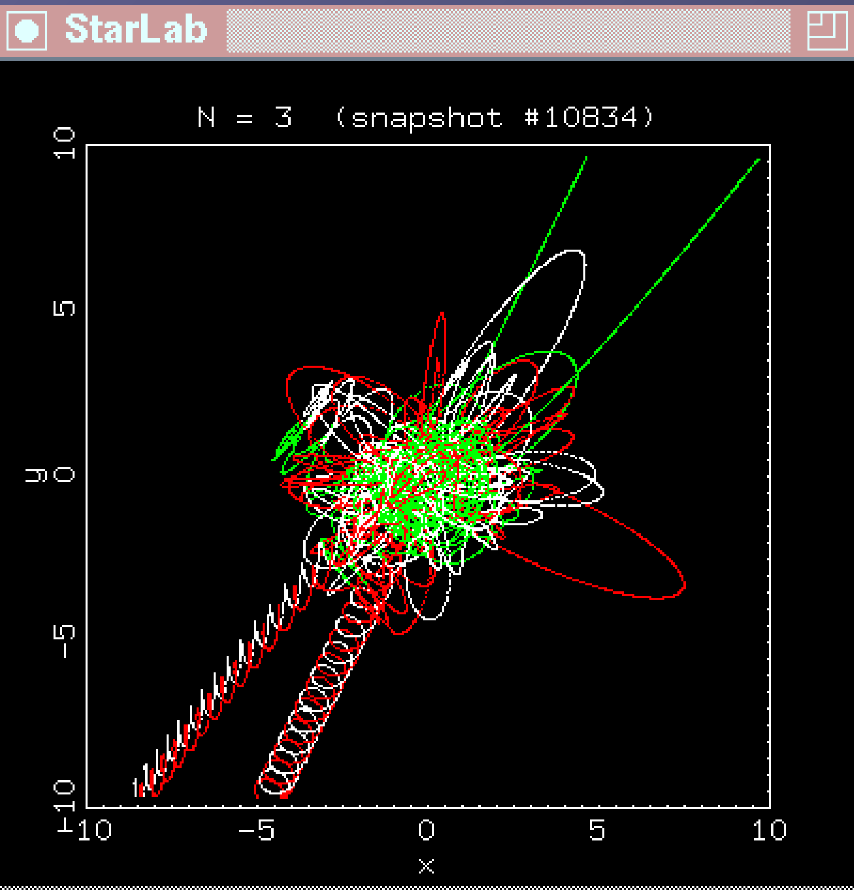


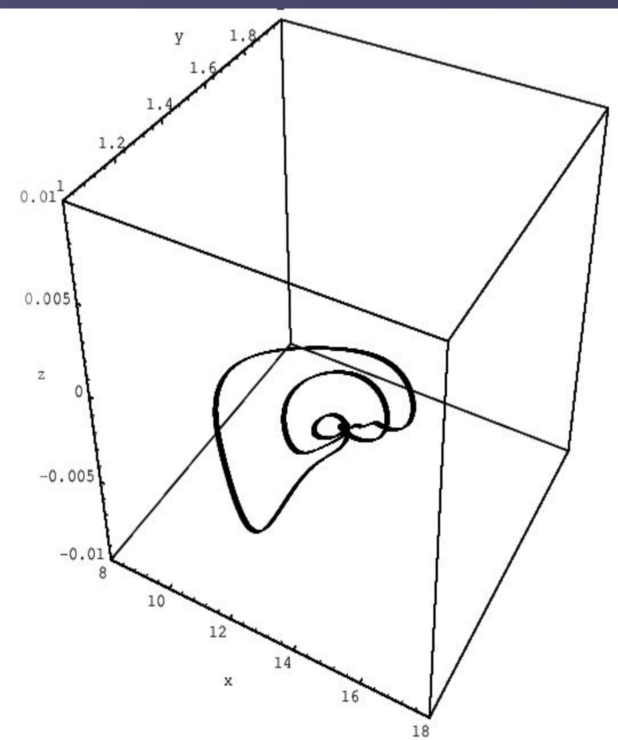


**Fig. 3:**
Projected three-dimensional attractor for $N = 100.000$ system, $x = \log \rho'_c$, $y = \log \sigma'_c$, $z = \xi$.

# Star Clusters: Modelling the Dynamics

## (multiple time scales)

- Millisecond Pulsars — $10^{-3}$ sec
- Dynamical Time Scale — $10^{6}$ yrs
- Relaxation Time Scale — $10^{8}$ yrs**
- Age of Universe — $10^{10}$ yrs

$$t_{\rm cr} = \frac{r_h}{\sigma_h} ,$$

$$t_{\rm rx} = \frac{9}{16\sqrt{\pi}} \frac{\sigma^3}{G^2 m \rho \ln(\gamma N)} .$$

**Laboratories for gravothermal N-Body Systems!**

Note: Cosmological and Galactic N-Body Simulations need few crossing times, and less than a relaxation time, while gravothermal systems need multiples of N crossing times, several … Complexity goes approx N**2.3 !

$$t_{\rm cr} \approx \sqrt{\frac{r_h^3}{G M_h}} .$$

← Virial Equilibrium →

$$\frac{t_{\rm rx}}{t_{\rm dyn}} \propto \frac{N}{\log(\gamma N)} .$$

Relaxation time definitions: Here: Larson, R.B. (1970) – theoretically sound, also see Spurzem & Takahashi (1995); in N-Body Code use: Eq. (8-71) of Binney/Tremaine (BT) Galactic Dynamics (from Spitzer & Hart 1971)

# Star Clusters: Modelling the Dynamics

(compare gaseous model with direct N-body integration)

(Spurzem & Aarseth 1996)

(Giersz & Spurzem 1994)
(now in Binney/Tremaine)

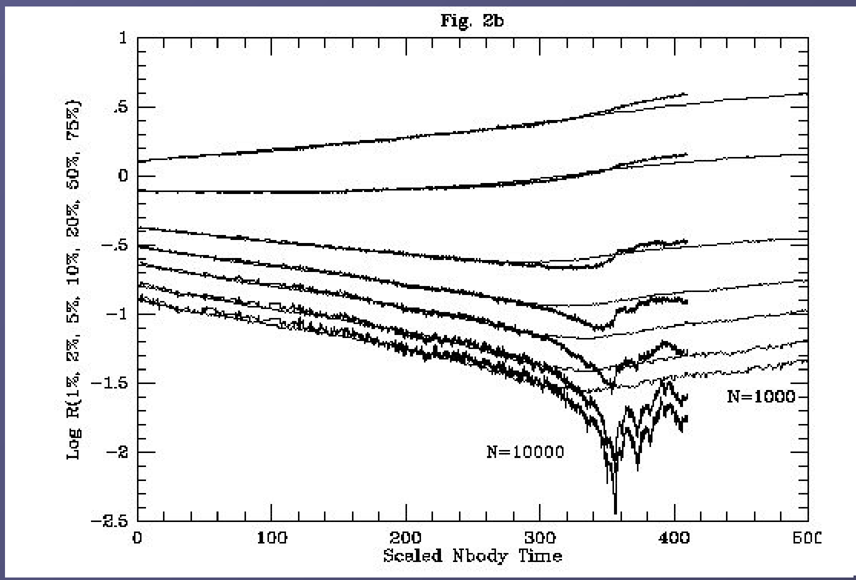


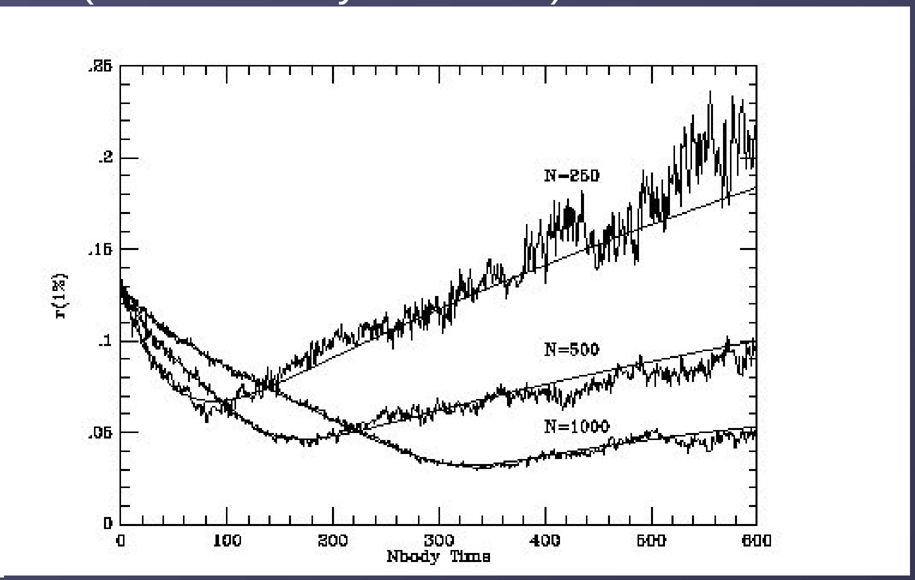


N-Body / N-Body

N-Body / Fokker-Planck

In spherical symmetry

...but...

Mon. Not. R. astr. Soc. (1980) 191, 483–498

# Star Clusters: Modelling the Dynamics

**On the consequences of the gravothermal catastrophe**

(all depends on the conductivity / viscosity)

D. Lynden-Bell and P. P. Eggleton *Institute of Astronom*
*The Observatories, Cambridge CB3 0HA*

**1980**

Received 1979 October 9; in original form 1979 July 11

$$\frac{L}{4\pi r^2} = -\rho \cdot \frac{\lambda^2}{\tau}\frac{\partial}{\partial r}\left(\frac{3}{2}\frac{kT}{m}\right),$$

between encounters. In such a stellar system a typical star at any radius moves in and out by about a local Jeans length $\lambda = 1/k_J$ where $k_J^2 v^2 = 4\pi G\rho$. This gives a typical radial distance between encounters. However, the time between those encounters is not $\lambda/v$ but rather a relaxation time $T_r$. Hence the energy flux is given by equation (3.5) with $\lambda = k_J^{-1}$ and with $\tau$ replaced by $T_r$

$$\frac{L}{4\pi r^2} = -\frac{C\rho}{k_J^2 T_r}\frac{\partial}{\partial r}\left(\frac{3}{2}v^2\right) \quad (3.7)$$

$$= -3GmC(\log N)\frac{\rho}{v}\frac{\partial v^2}{\partial r} \quad (3.8)$$

- Conductivity ∝ ρ/v = $\rho T^{-1/2}$
- Based on Jeans Length
- Later: very general

where $C$ is a dimensionless constant of order unity. As Lecar pointed out, this implies a conductivity $K$ proportional to $\rho T^{-1/2}$ or an opacity $\kappa$ proportional to $T^{3.5}\rho^{-2}$. Notice that the details of the argument are unimportant, for the use of dimensions, coupled with the fact that the heat flux must be proportional to the relaxation rate ($T_r^{-1}$) gives the same dependence of conductivity on $\rho, v$. The detailed computation of Hachisu *et al.* (1978) was

1) Introduction, History, Theory

**<u>2) Star Cluster Dynamics with Black Holes and Gravitational Waves</u>**

3) Nuclear Star Clusters

4) People, Code(s) and Hardware

5) Summary and References

# DRAGON I Simulation

# DRAGON Simulation

https://astro-silkroad.eu
https://github.com/nbody6ppgpu
**Also in:** https://www.punch4nfdi.de/

***One million stars direct simulation,***

biggest and most realistic direct N-Body simulation of globular star clusters.

With stellar mass function, single and binary stellar evolution, regularization of close encounters, tidal field (NBODY6++GPU).

***(NAOC/Silk Road/MPA collaboration).***

Wang, Spurzem, Aarseth, Naab et al.
MNRAS, 2015
Wang, Spurzem, Aarseth Naab, et al.
MNRAS 2016

Number of Floating Point Operations (~1M bodies) similar to largest Cosmological simulations (Millennium, Illustris, ~$10^{10}$ bodies)

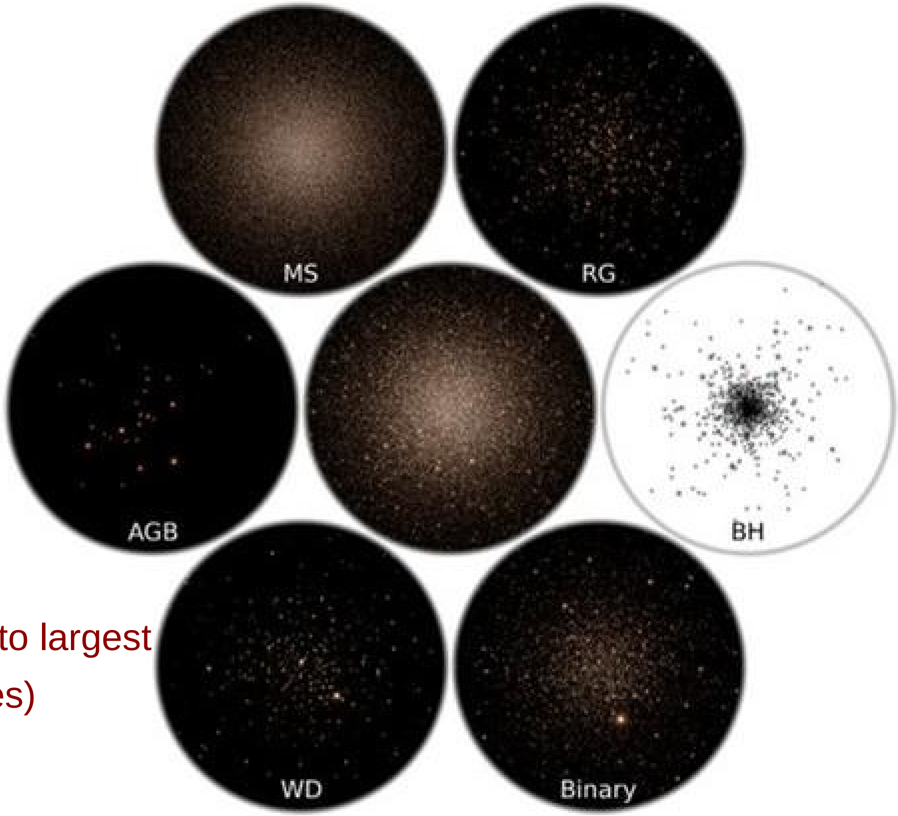

# 天龙星团模拟：百万数量级恒星、黑洞和引力波

## Dragon Star Cluster Simulations: Millions of Stars; black holes and gravitational waves

- **First realistic globular star cluster model with million stars *(Wang, Spurzem, Aarseth, …, Berczik, Kouwenhoven, … MNRAS 2015, 2016)***
- **Synthetic CMD (right side) with zero photometric errors, different ages shown**
- **Black hole binary mergers occur as observed by LIGO. Our grav. waveforms computed from simulation (right side). (Only inspiral plotted not ringdown.)**
- **GPU accelerated supercomputers laohu in NAOC and hydra of Max-Planck (MPCDF) in Germany needed!**

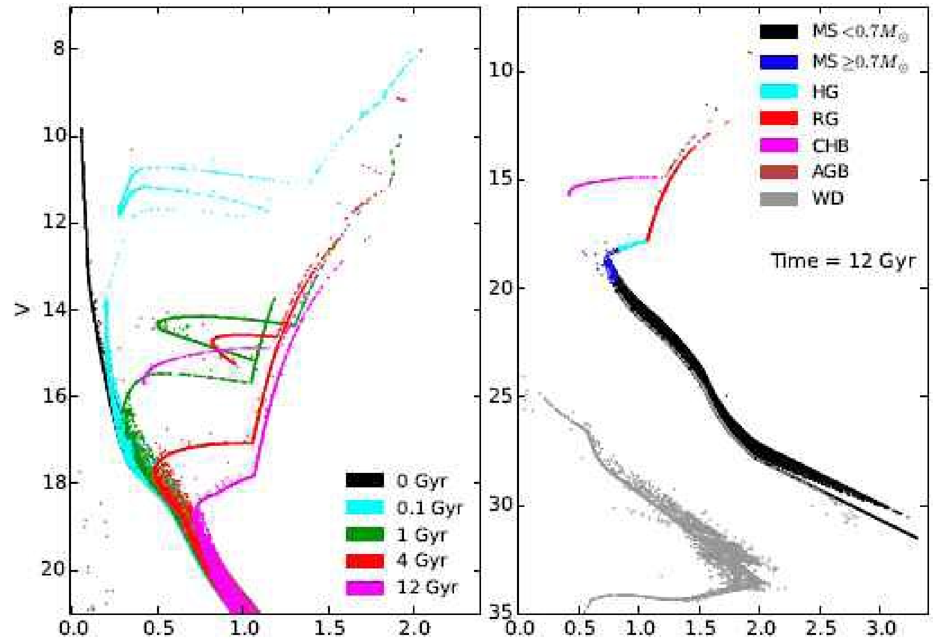



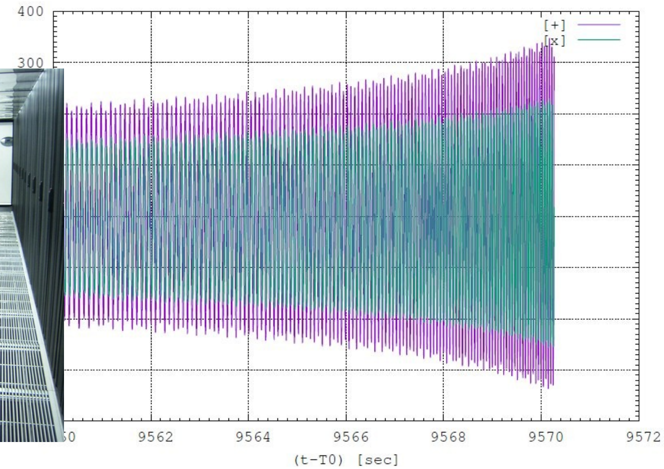


http://www.mpa-garching.mpg.de/328833/hl201603

What about black holes?
Black Hole Binaries?
DRAGON II Models

# Black Holes were retained in globular clusters simulations (and formed binaries, gravitational wave emission predicted 2010):

- **Before Strader et al. detection**
- **Before Breen & Heggie**
- **Before LIGO detection**

Downing 2012, Downing, Benacquista, Giersz & Spurzem, 2010, 2011:
(see also Banerjee, Baumgardt & Kroupa 2010 but … )

## Compact Binaries in Star Clusters I - Black Hole Binaries Inside Globular Clusters

J. M. B. Downing[3⋆], M. Benacquista[4], R. Spurzem[1,2,3], and M. Giersz[5]
[1] National Astronomical Observatories, Chinese Academy of Sciences, 20A Datun Ln, Chaoyang District, 100012, China
[2] Kavli Institute of Astronomy and Astrophysics, Peking University, Beijing, China
[3] Astronomisches Rechen-Institut, Zentrum für Astronomie der Universität Heidelberg, Monchhofsraße 12-14, D-69120 Heidelberg, Germany
[4] Center for Gravitational Wave Astronomy, University of Texas at Brownsville, Brownsville, TX 78520, USA
[5] Nicolaus Copernicus Astronomical Center, Polish Academy of Sciences, ul. Bartycka 18, 00-716 Warsaw, Poland

## Compact Binaries in Star Clusters II - Escapers and Detection Rates

J. M. B. Downing[1,2⋆], M. J. Benacquista[3], M. Giersz[4], and R. Spurzem[5,6,1]
[1] Astronomisches Rechen-Institut, Zentrum für Astronomie der Universität Heidelberg, Monchhofsraße 12-14, D-69120 Heidelberg, Germany
[2] Fellow of the International Max-Planck Research School for Astronomy and Cosmic Physics at the University of Heidelberg, Heidelberg, Germany
[3] Center for Gravitational Wave Astronomy, University of Texas at Brownsville, Brownsville, TX 78520, USA
[4] Nicolaus Copernicus Astronomical Center, Polish Academy of Sciences, ul. Bartycka 18, 00-716 Warsaw, Poland
[5] National Astronomical Observatories, Chinese Academy of Sciences, 20A Datun Rd., Chaoyang District, 100012, China
[6] Kavli Institute of Astronomy and Astrophysics, Peking University, Beijing, China

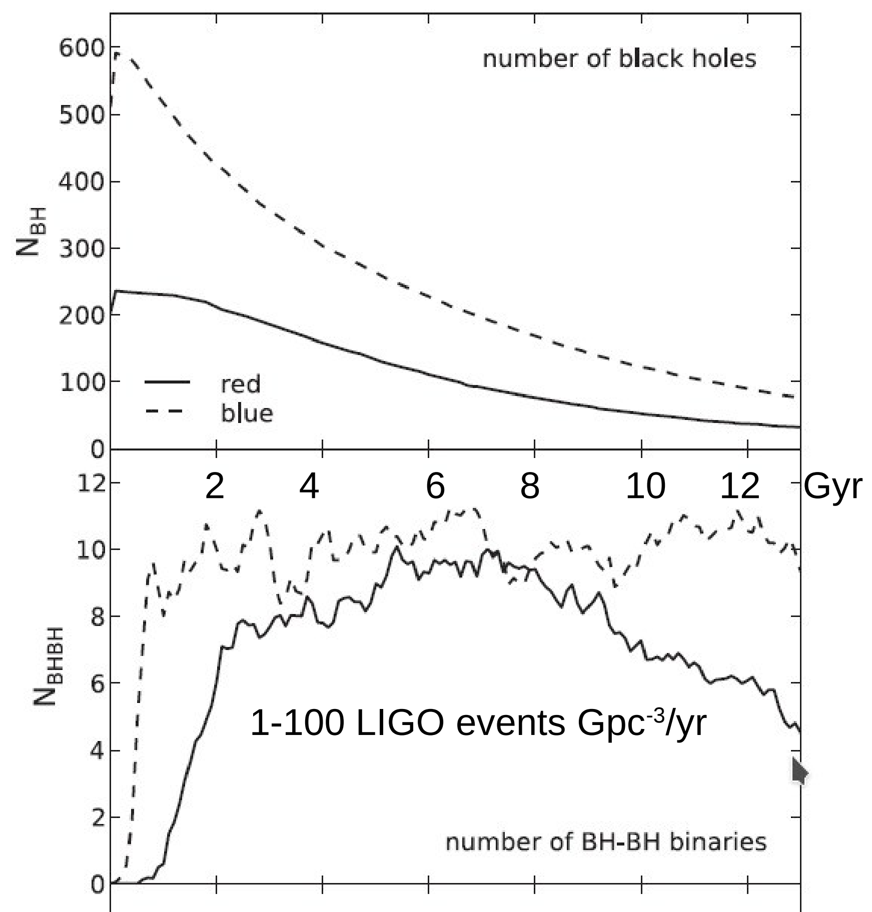

# Post-Newtonian Dynamics

**r;v** : relative distance, velocity

μ = $m_1 m_2/M$ : reduced mass ( $M = m_1 + m_2$ )

ν = μ / M : mass ratio

**n** = **r** / r : unit vector in radial direction

$$\frac{dv^i}{dt} = -\frac{Gm}{r^2}\left[(1+\mathcal{A})\,n^i + \mathcal{B}\,v^i\right] + \mathcal{O}\left(\frac{1}{c^8}\right), \tag{181}$$

and find [43] that the coefficients $\mathcal{A}$ and $\mathcal{B}$ are

$$\begin{aligned}\mathcal{A} = {} & \frac{1}{c^2}\left\{-\frac{3\dot{r}^2\nu}{2} + v^2 + 3\nu v^2 - \frac{Gm}{r}(4+2\nu)\right\} \\ & + \frac{1}{c^4}\left\{\frac{15\dot{r}^4\nu}{8} - \frac{45\dot{r}^4\nu^2}{8} - \frac{9\dot{r}^2\nu v^2}{2} + 6\dot{r}^2\nu^2 v^2 + 3\nu v^4 - 4\nu^2 v^4\right. \\ & \left. + \frac{Gm}{r}\left(-2\dot{r}^2 - 25\dot{r}^2\nu - 2\dot{r}^2\nu^2 - \frac{13\nu v^2}{2} + 2\nu^2 v^2\right) + \frac{G^2m^2}{r^2}\left(9 + \frac{87\nu}{4}\right)\right\} \\ & + \frac{1}{c^5}\left\{-\frac{24\dot{r}\nu v^2}{5}\frac{Gm}{r} - \frac{136\dot{r}\nu}{15}\frac{G^2m^2}{r^2}\right\}\end{aligned}$$

Perihel shift

... higher order…

Grav. Radiation

Schäfer, Gauge Theor. Grav. 36, 2223 (2004)

Memmesheimer, Gopakumar, Schäfer, Phys. Rev.D 70, 104011 (2004)

Blanchet, Luc; Living Reviews 2002, llr-2002-3

$$
\begin{aligned}
&+\frac{1}{c^6}\left\{-\frac{35\dot{r}^6\nu}{16}+\frac{175\dot{r}^6\nu^2}{16}-\frac{175\dot{r}^6\nu^3}{16}+\frac{15\dot{r}^4\nu v^2}{2}-\frac{135\dot{r}^4\nu^2v^2}{4}+\frac{255\dot{r}^4\nu^3v^2}{8}\right.\\
&\quad-\frac{15\dot{r}^2\nu v^4}{2}+\frac{237\dot{r}^2\nu^2v^4}{8}-\frac{45\dot{r}^2\nu^3v^4}{2}+\frac{11\nu v^6}{4}-\frac{49\nu^2v^6}{4}+13\nu^3v^6\\
&\quad+\frac{Gm}{r}\left(79\dot{r}^4\nu-\frac{69\dot{r}^4\nu^2}{2}-30\dot{r}^4\nu^3-121\dot{r}^2\nu v^2+16\dot{r}^2\nu^2v^2+20\dot{r}^2\nu^3v^2+\frac{75\nu v^4}{4}\right.\\
&\qquad\left.+8\nu^2v^4-10\nu^3v^4\right)\\
&\quad+\frac{G^2m^2}{r^2}\left(\dot{r}^2+\frac{32573\dot{r}^2\nu}{168}+\frac{11\dot{r}^2\nu^2}{8}-7\dot{r}^2\nu^3+\frac{615\dot{r}^2\nu\pi^2}{64}-\frac{26987\nu v^2}{840}+\nu^3v^2\right.\\
&\qquad\left.-\frac{123\nu\pi^2v^2}{64}-110\dot{r}^2\nu\ln\left(\frac{r}{r_0'}\right)+22\nu v^2\ln\left(\frac{r}{r_0'}\right)\right)\\
&\quad\left.+\frac{G^3m^3}{r^3}\left(-16-\frac{437\nu}{4}-\frac{71\nu^2}{2}+\frac{41\nu\pi^2}{16}\right)\right\}\\
&+\frac{1}{c^7}\left\{\frac{Gm}{r}\left(\frac{366}{35}\nu v^4+12\nu^2v^4-114v^2\nu\dot{r}^2-12\nu^2v^2\dot{r}^2+112\nu\dot{r}^4\right)\right.\\
&\quad+\frac{G^2m^2}{r^2}\left(\frac{692}{35}\nu v^2-\frac{724}{15}v^2\nu^2+\frac{294}{5}\nu\dot{r}^2+\frac{376}{5}\nu^2\dot{r}^2\right)\\
&\quad\left.+\frac{G^3m^3}{r^3}\left(\frac{3956}{35}\nu+\frac{184}{5}\nu^2\right)\right\},
\end{aligned}
\tag{182}
$$

$$
\begin{aligned}
\mathcal{B} = {}& \frac{1}{c^2}\left\{-4\dot{r} + 2\dot{r}\nu\right\} \\
&+ \frac{1}{c^4}\left\{\frac{9\dot{r}^3\nu}{2} + 3\dot{r}^3\nu^2 - \frac{15\dot{r}\nu v^2}{2} - 2\dot{r}\nu^2 v^2 + \frac{Gm}{r}\left(2\dot{r} + \frac{41\dot{r}\nu}{2} + 4\dot{r}\nu^2\right)\right\} \\
&+ \frac{1}{c^5}\left\{\frac{8\nu v^2}{5}\frac{Gm}{r} + \frac{24\nu}{5}\frac{G^2m^2}{r^2}\right\} \\
&+ \frac{1}{c^6}\left\{-\frac{45\dot{r}^5\nu}{8} + 15\dot{r}^5\nu^2 + \frac{15\dot{r}^5\nu^3}{4} + 12\dot{r}^3\nu v^2 - \frac{111\dot{r}^3\nu^2 v^2}{4} - 12\dot{r}^3\nu^3 v^2 - \frac{65\dot{r}\nu v^4}{8}\right. \\
&\qquad + 19\dot{r}\nu^2 v^4 + 6\dot{r}\nu^3 v^4 \\
&\qquad + \frac{Gm}{r}\left(\frac{329\dot{r}^3\nu}{6} + \frac{59\dot{r}^3\nu^2}{2} + 18\dot{r}^3\nu^3 - 15\dot{r}\nu v^2 - 27\dot{r}\nu^2 v^2 - 10\dot{r}\nu^3 v^2\right) \\
&\qquad \left. + \frac{G^2m^2}{r^2}\left(-4\dot{r} - \frac{18169\dot{r}\nu}{840} + 25\dot{r}\nu^2 + 8\dot{r}\nu^3 - \frac{123\dot{r}\nu\pi^2}{32} + 44\dot{r}\nu\ln\left(\frac{r}{r'_0}\right)\right)\right\} \\
&+ \frac{1}{c^7}\left\{\frac{Gm}{r}\left(-\frac{626}{35}\nu v^4 - \frac{12}{5}\nu^2 v^4 + \frac{678}{5}\nu v^2\dot{r}^2 + \frac{12}{5}\nu^2 v^2\dot{r}^2 - 120\nu\dot{r}^4\right)\right. \\
&\qquad + \frac{G^2m^2}{r^2}\left(\frac{164}{21}\nu v^2 + \frac{148}{5}\nu^2 v^2 - \frac{82}{3}\nu\dot{r}^2 - \frac{848}{15}\nu^2\dot{r}^2\right) \\
&\qquad \left. + \frac{G^3m^3}{r^3}\left(-\frac{1060}{21}\nu - \frac{104}{5}\nu^2\right)\right\}. \qquad (183)
\end{aligned}
$$

# Indirect Proof by Hulse and Taylor, binary pulsar (Nobel prize 1993)


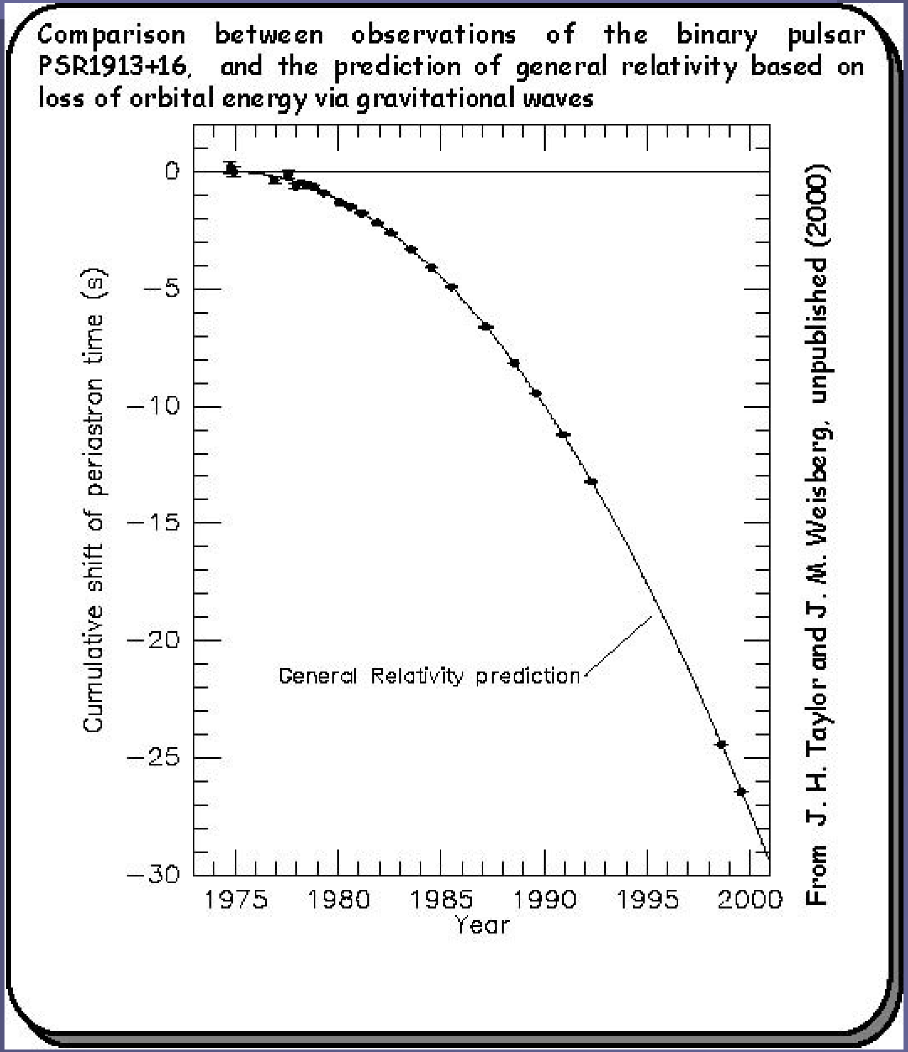

# Gravitational Waves

## What happens afterwards? Post-Newton Order „2.5"...

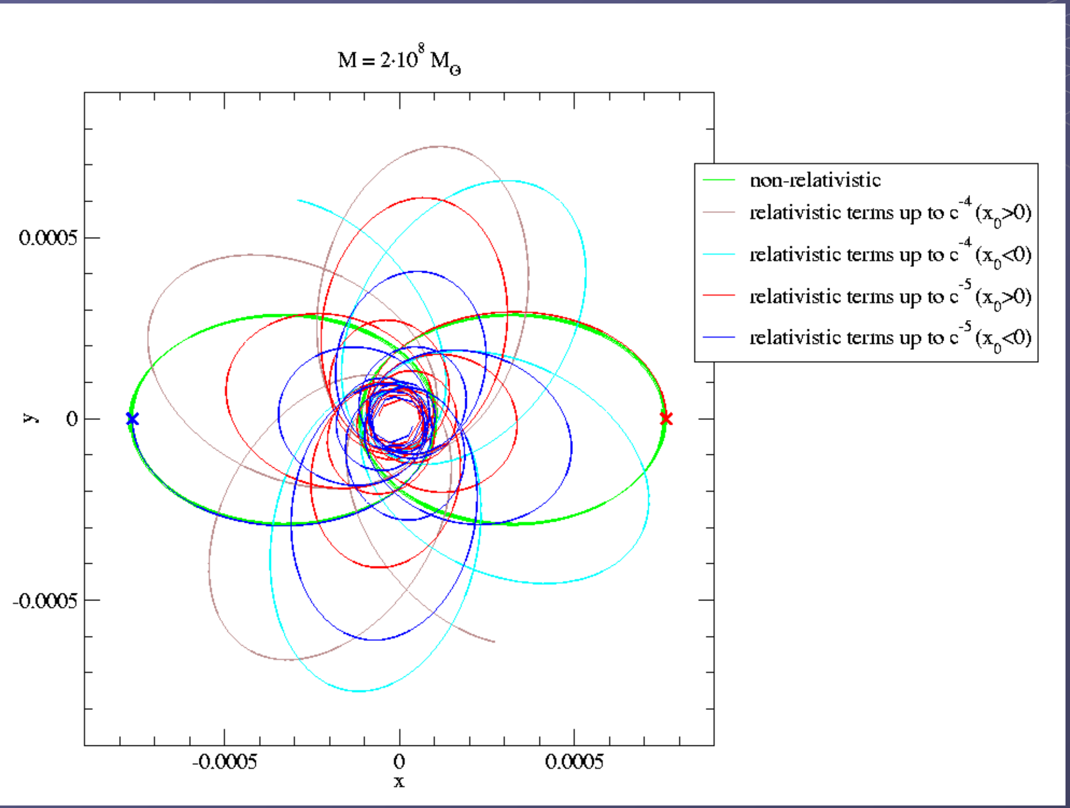


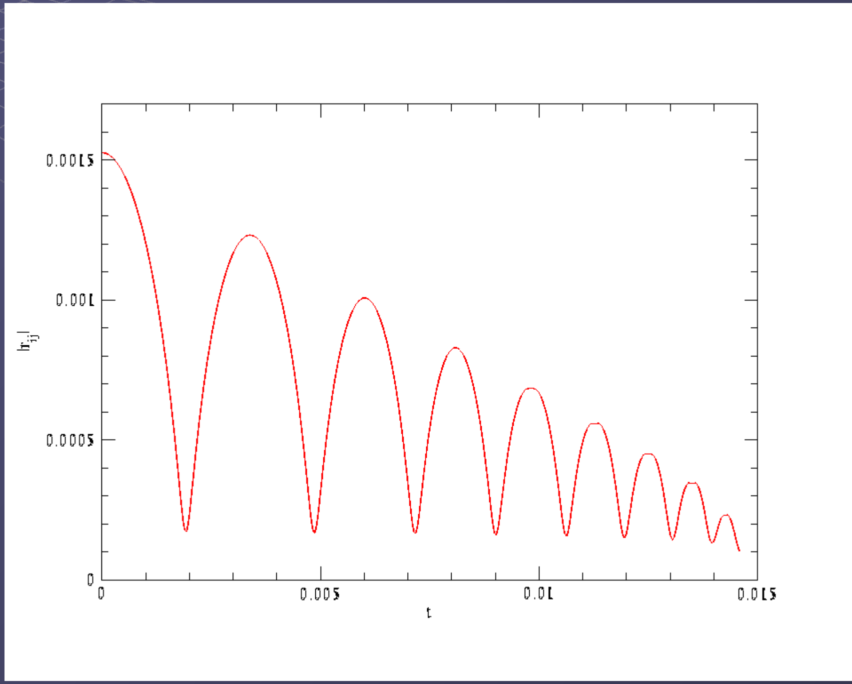


Kupi, Amaro-Seoane & Spurzem 2006

# Post-Newtonian Dynamics Gravitational Wave Templates

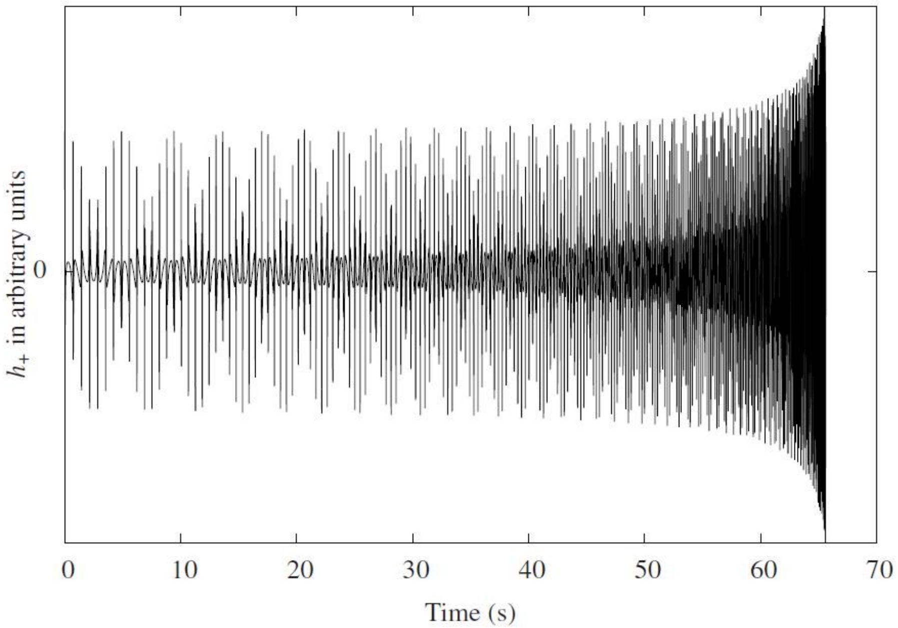


Figure 3.11: Waveform for two equal mass objects on a an orbit with $e = 0.5$.

Brem,
Amaro-Seoane,
Spurzem,
MNRAS 2013

Handle spin-orbit and spin-spin coupling
(P.Brem, R. Spurzem, Univ. Heidelberg)

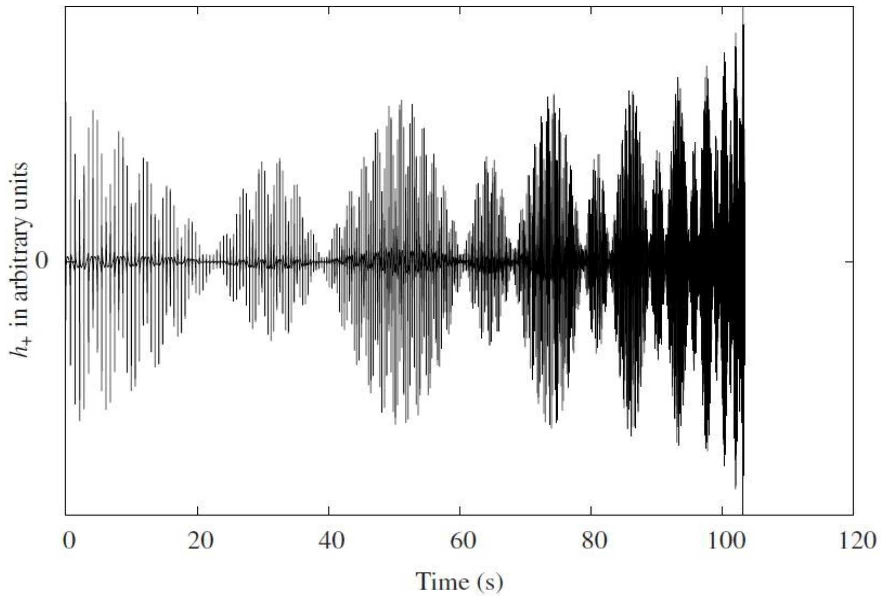


Figure 3.12: Waveform for two objects with a mass ratio of $q = 1/10$ on an orbit with $e = 0.5$ and spins $a_{1,x} = 1.0$, $a_{2,y} = 1.0$.


VIRGO Detector in Cascina near Pisa, Italy
(LIGO USA, KAGRA Japan)

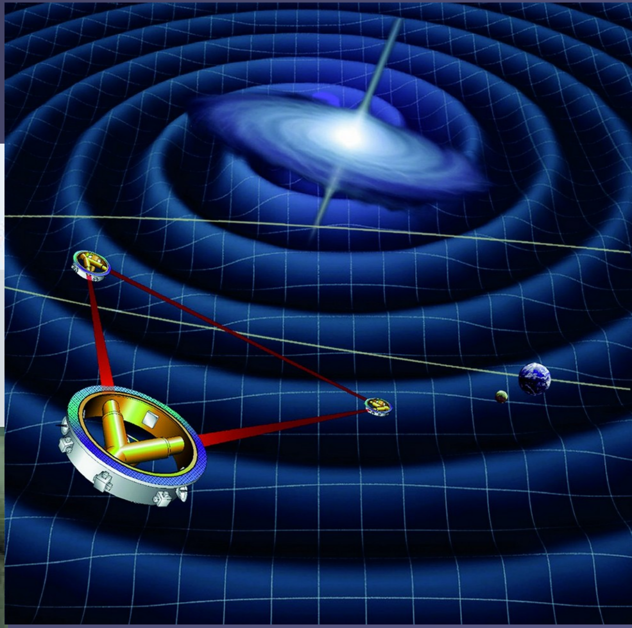

LISA =
Laser Space
Interferometer Antenna

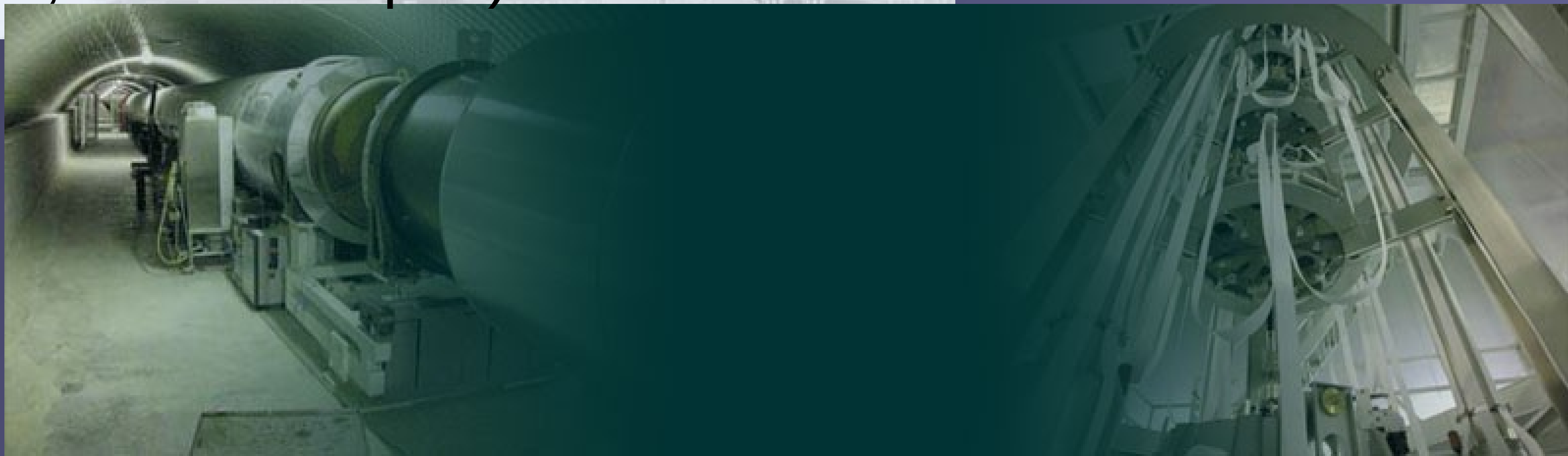

# GW Detection Abott et al. 2016

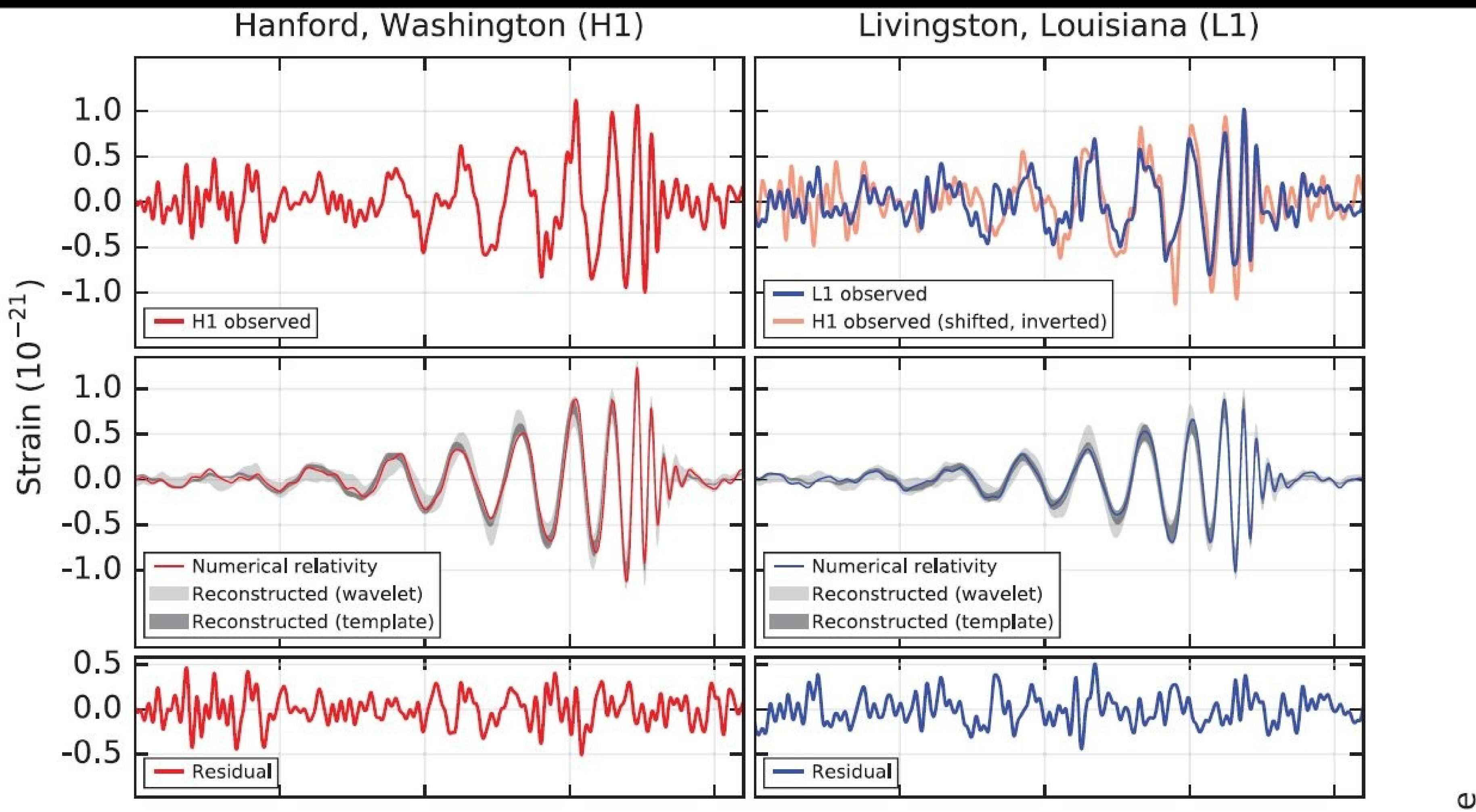

# Masses in the Stellar Graveyard

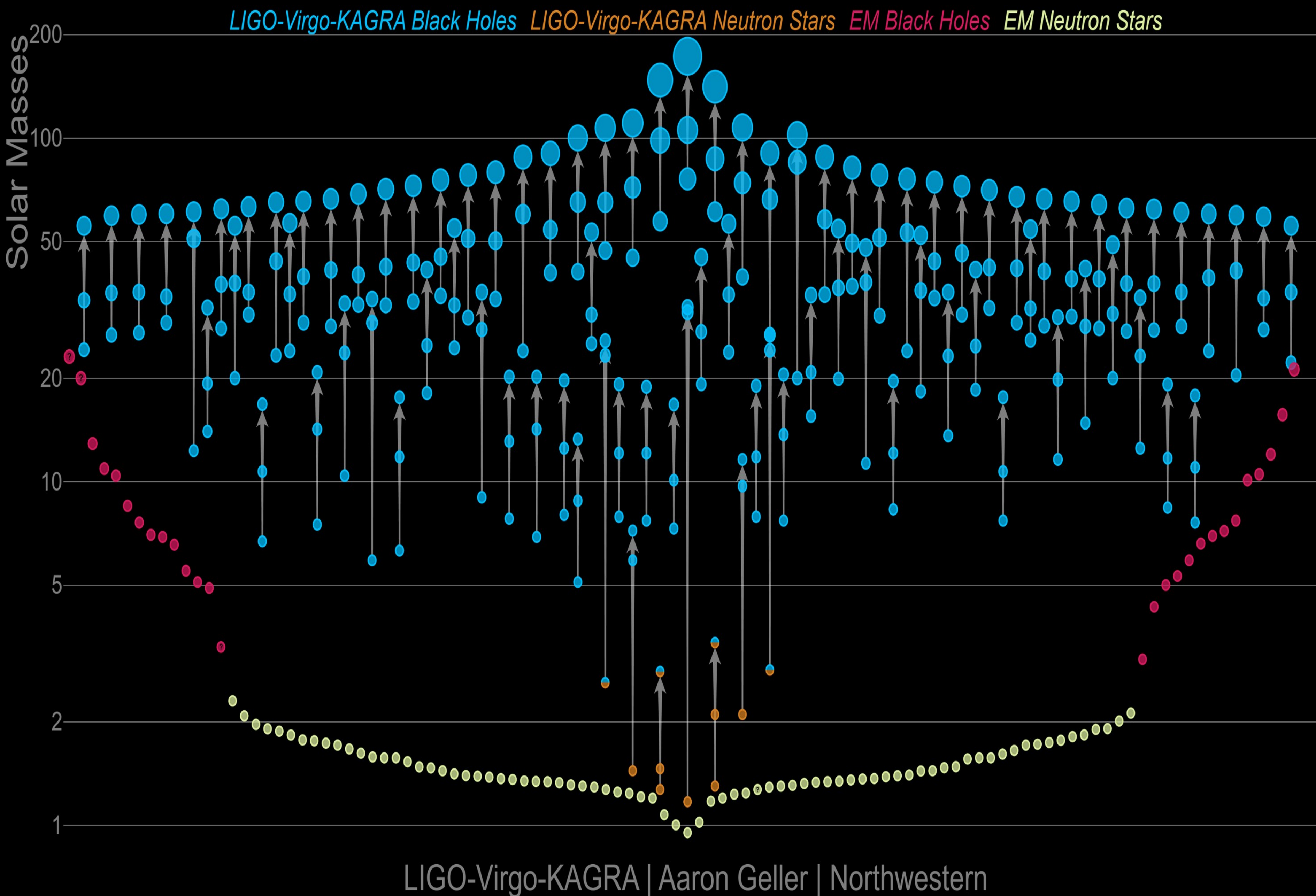

# DRAGON-II Simulations

## using NBODY6++GPU

$$\left\langle \frac{da}{dt} \right\rangle = -\frac{64}{5} \frac{G^3 m_1 m_2 (m_1+m_2)}{c^5 a^3 (1-e^2)^{7/2}} \left(1 + \frac{73}{24} e^2 + \frac{37}{96} e^4 \right),$$

$$\left\langle \frac{de}{dt} \right\rangle = -\frac{304}{15} e \frac{G^3 m_1 m_2 (m_1+m_2)}{c^5 a^4 (1-e^2)^{5/2}} \left(1 + \frac{121}{304} e^2 \right).$$

Orbit Averaged Post-Newtonian

evolution of

semi-major axis a, eccentricity e

(Peters & Mathews 1963,

Peters 1964)

$$\begin{aligned}
\vec{v}_{GW} &= v_m \hat{e}_{\perp,1} + v_\perp (\cos\xi \hat{e}_{\perp,1} + \sin\xi \hat{e}_{\perp,2}) + v_\parallel \hat{e}_\parallel, \\
v_m &= A\eta^2 \sqrt{1-4\eta}(1+B\eta), \\
v_\perp &= \frac{H\eta^2}{1+q_{BBH}} \left( S_{2,\parallel} - q_{BBH} S_{1,\parallel} \right), \\
v_\parallel &= \frac{16\eta^2}{1+q_{BBH}} \left[ V_{11} + V_A \Xi_\parallel + V_B \Xi_\parallel^2 + V_C \Xi_\parallel^3 \right] \times \\
&\quad \times \left| \vec{S}_{2,\perp} - q_{BBH} \vec{S}_{1,\perp} \right| \cos(\phi_\Delta - \phi_1).
\end{aligned}$$

Black Hole Binary Mergers

with relativistic kicks

including spins

(DRAGON II,

Arca Sedda et al. 2023ab, 2024)

# DRAGON-II Simulations – Paper II

## using NBODY6++GPU

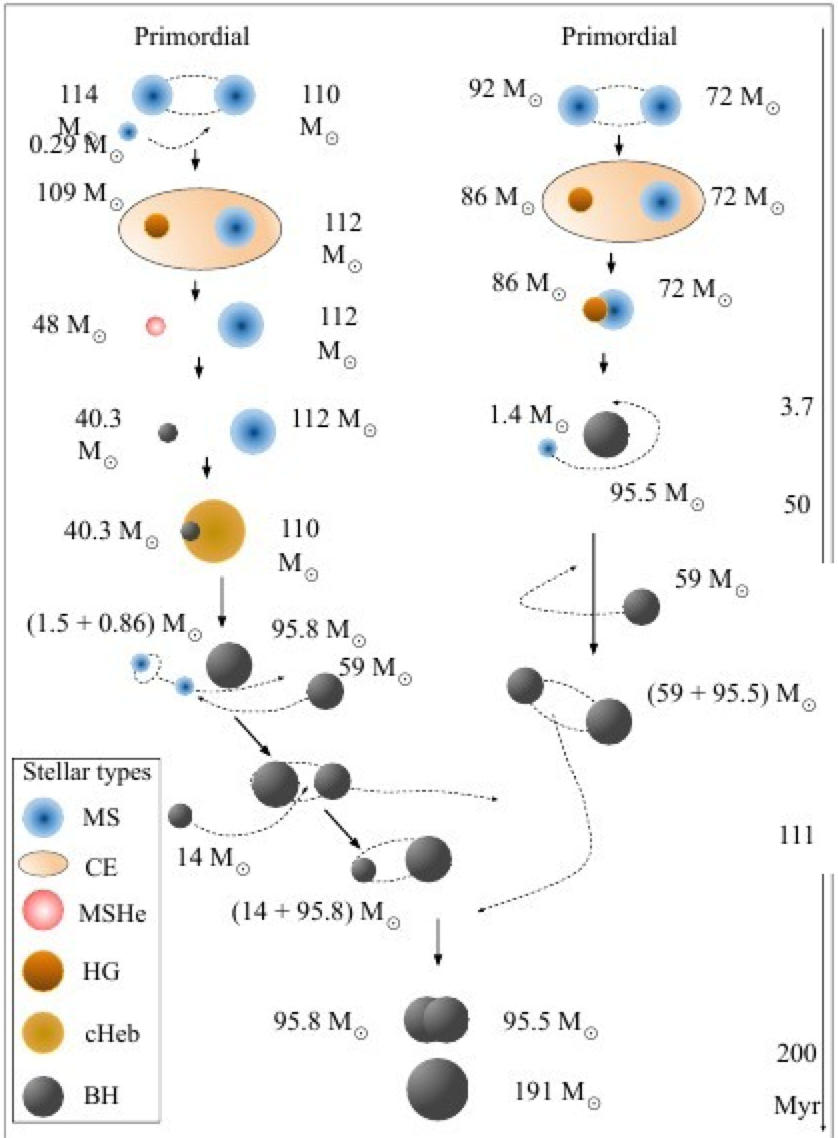


*Arca Sedda et al. 2023abc: MNRAS:*

*19 models, up to 1 million stars, up to 33% initial hard binaries*

***Including GR kicks for mergers!***

**Figure 2.** Formation of an IMBH in simulation with $N = 120$k, $R_{\rm HM} = 1.75$ pc, and $f_b = 0.2$, realization ID 0. Two massive primordial binaries undergo common envelope that eventually lead to the formation of two nearly equal mass BHs ($m_{\rm BH} \sim 95$ M$_\odot$) that eventually find each other via a complex series of binary-binary interactions. The binary eventually merge and builds-up an IMBH with mass $m_{\rm IMBH} \simeq 191$ M$_\odot$. The color-coded legend is ent colors correspond to different evolutionary stages: main sequence (MS), common envelope (CE), naked main sequence He star (MSHe), Hertzsprung gap (HG), core He burning (cHeb), and black hole (BH).

How DRAGON-II

Black Hole Binaries

Grav. Wave Emission

Could be observed?

(DRAGONII Papers,

ArcaSedda et al. 2023ab, 2024)

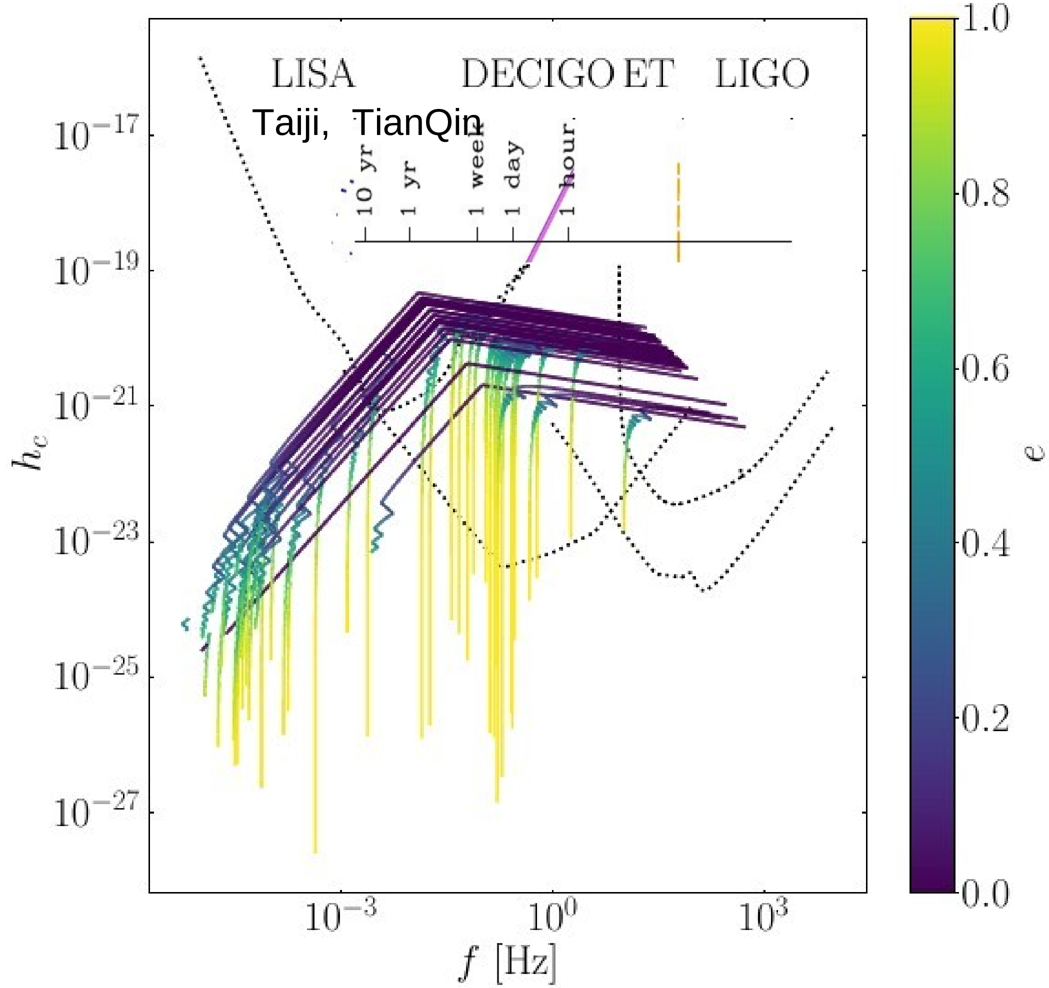


Fig.: ArcaSedda et al. 2023c;

Time Axis: Sesana et al. 2016

**Figure 7.** Evolution of the binary GW strain as a function of the frequency for all mergers in DRAGON-II simulations, assuming that the sources are located at a redshift $z = 0.05$. The colormap identifies the binary eccentricity along its orbit. Dotted lines represent sensitivity curves for different detectors, from left to right: LISA, DECIGO, ET, and LIGO.

# DRAGON-II Simulations – Paper III

## using NBODY6++GPU

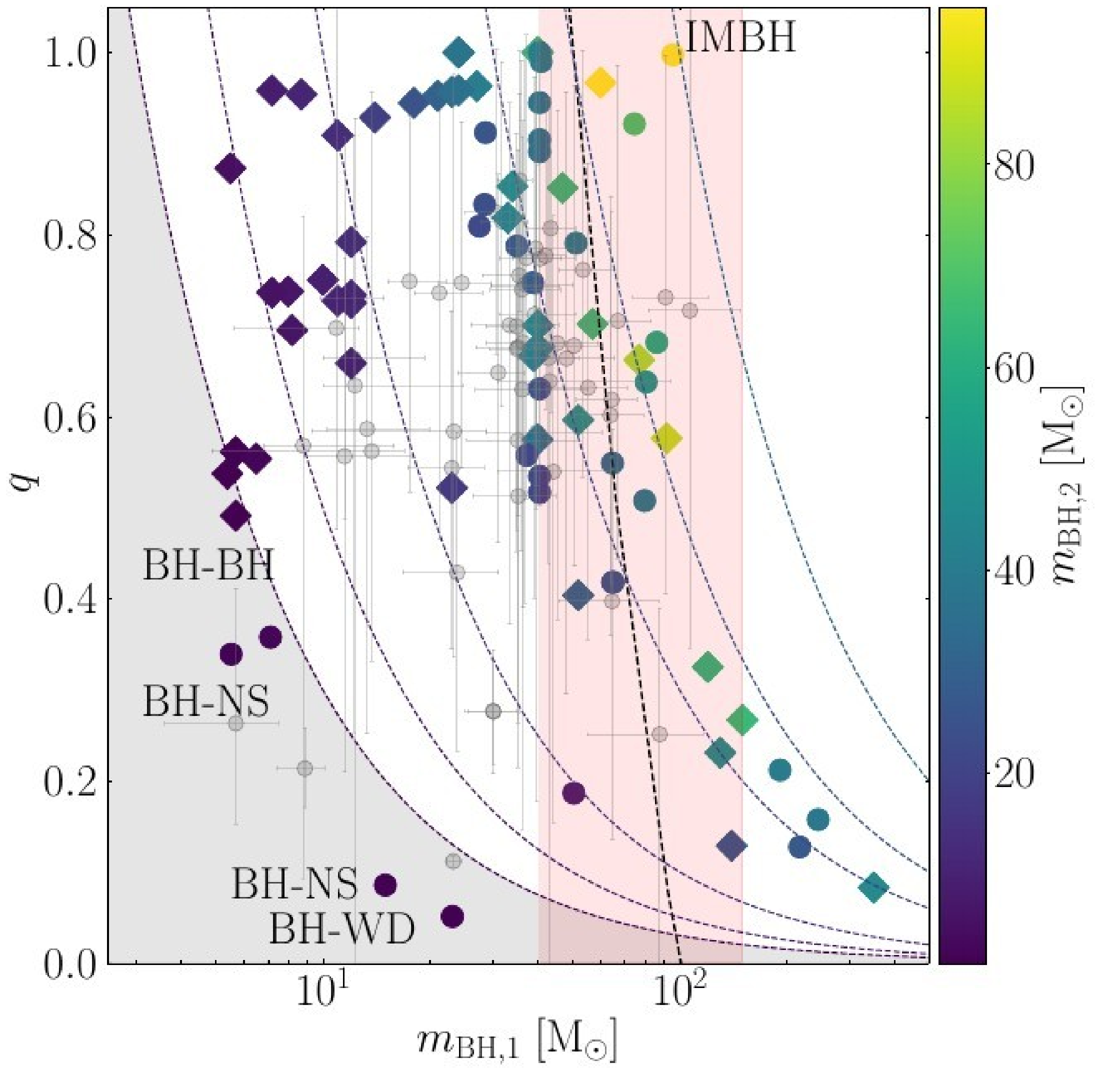


*Arca Sedda et al. 2023ab, 2024: MNRAS*

*19 models, up to 1 million stars, up to 33% initial hard binaries*

Compact Object Mergers

Compared with LIGO-Virgo GWTC-3 catalogue (grey symbols)

Mass ratio q vs. primary mass m1; colour code:

secondary mass m2

grey shade: neutron star involved

red Shade: mass gap

1) Introduction, History, Theory

2) Star Cluster Dynamics with
 Black Holes and Gravitational Waves

**3) Nuclear Star Clusters**

4) People, Code(s) and Hardware

5) Summary and References

# Setting the stage: the galactic nucleus

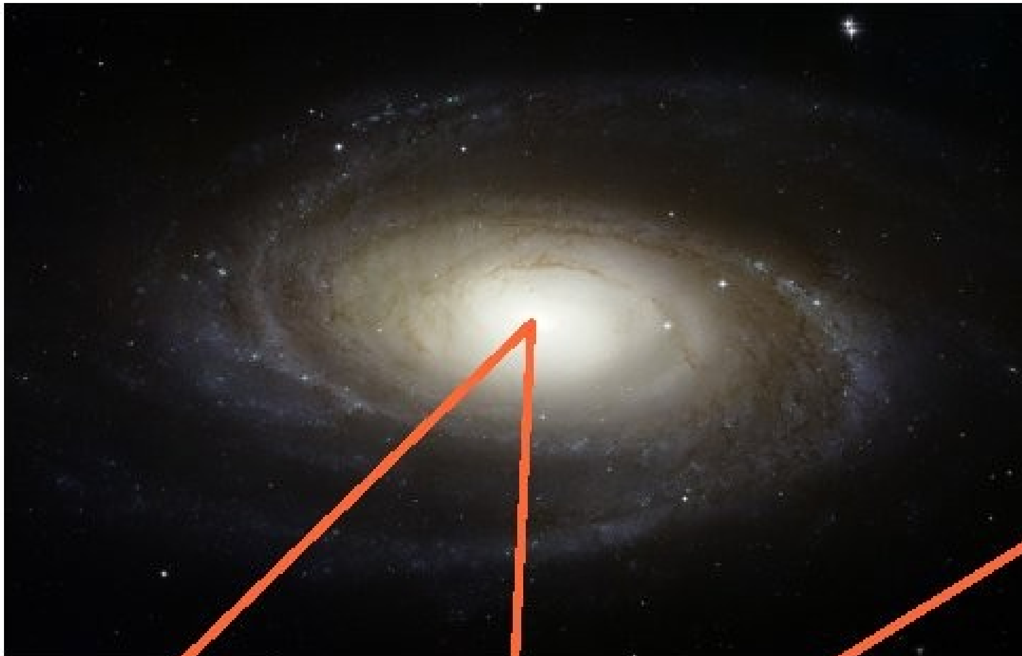

Size ~ 10 Kpc

Density ~ 0.05 $M_{sun}$ $pc^{-3}$

Vel. Disp. ~ 40 Km/s

Relaxation time ~ $10^{15}$ yrs.


Size ~ 1-10 pc

Density ~ $10^{6-8}$ $M_{sun}$ $pc^{-3}$

Vel. Disp. ~ $10^{2-3}$ Km/s

Relaxation time ~ $10^{8-9}$ yrs.

Size ~ $10^{-7}$-$10^{-4}$ pc

$R_s = 2G\, M_{BH}/c^2$

$R_t \sim (\alpha\, M_{BH}/m_*)^{1/3} R_*$

Loss cone aperture: $\theta$

*Slide: Miguel Preto*

# Distribution of stars

**Model: Panamarev, Just, Spurzem, Berczik, Wang, Arca Sedda 2019, MNRAS**

**“DRAGON” of Galactic Center (one million bodies, SMBH, 1% hard binaries)**

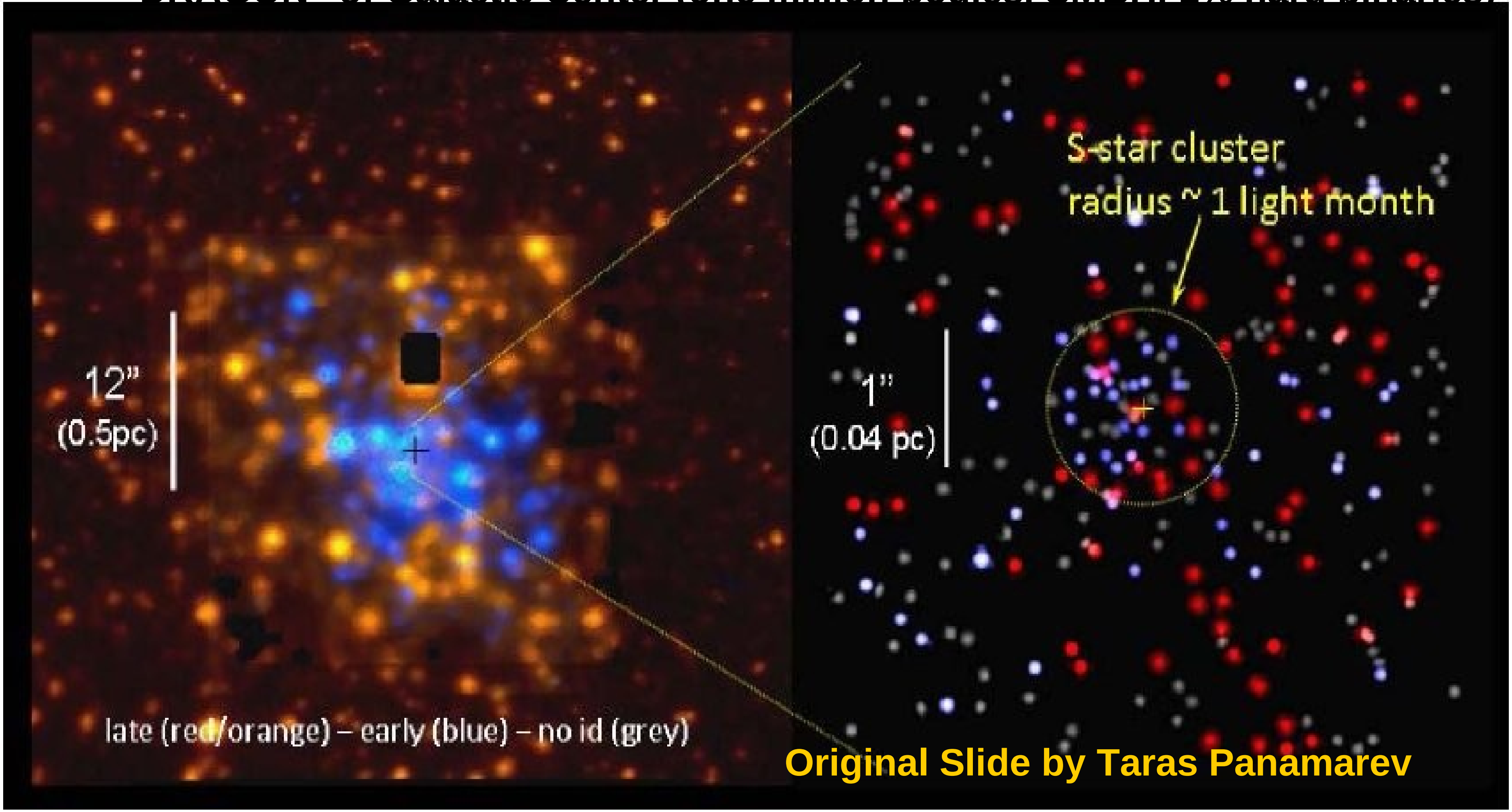


**Original Slide by Taras Panamarev**

# Black Holes in Galaxies

Stars moving
Around the
Central black
Hole in our Galaxy

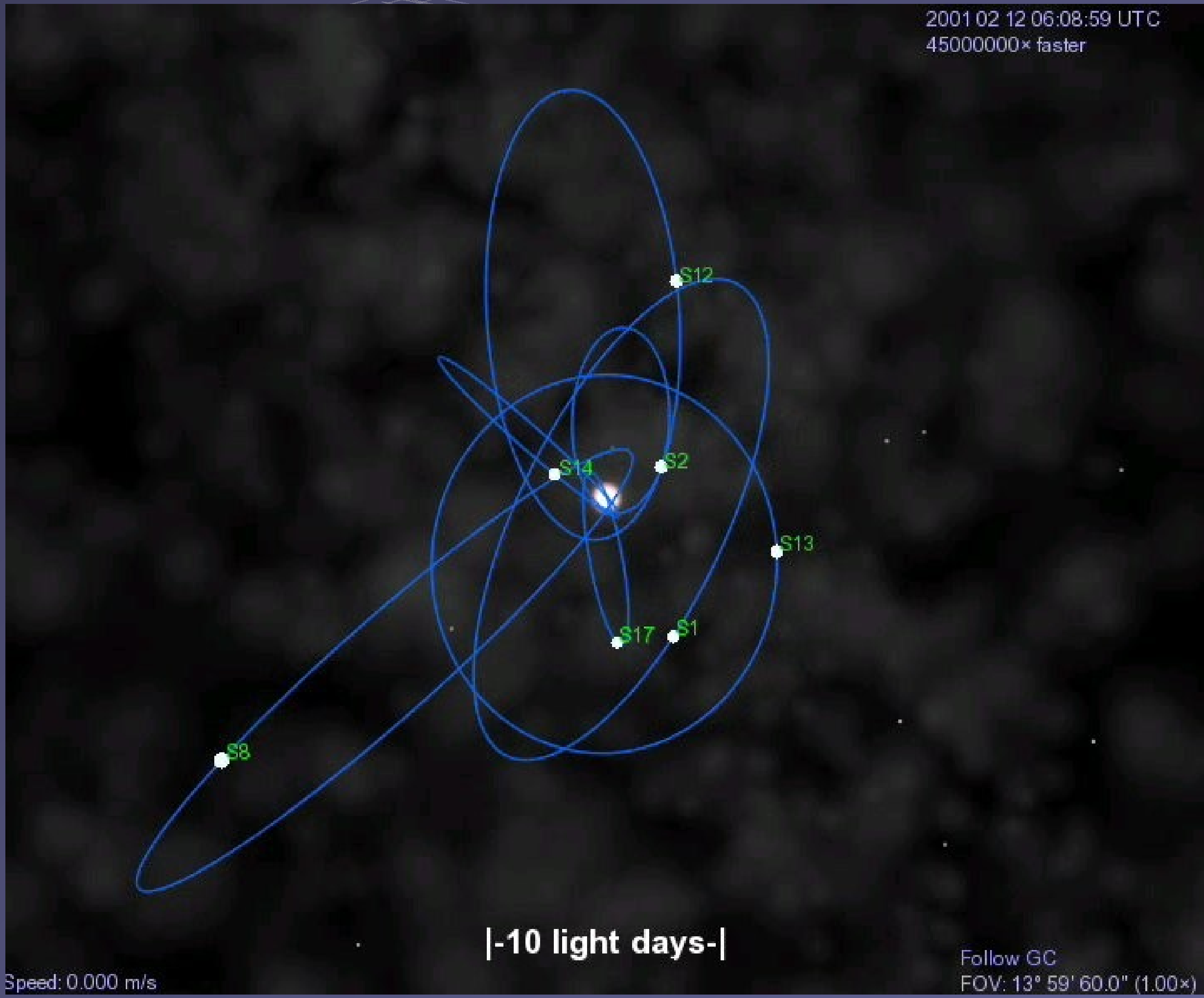


Max-Planck Inst.
Extraterrestrische
Physik Garching
http://www.mpe.mpg.de/ir/GC/

# DRAGON I Galactic Center Simulations

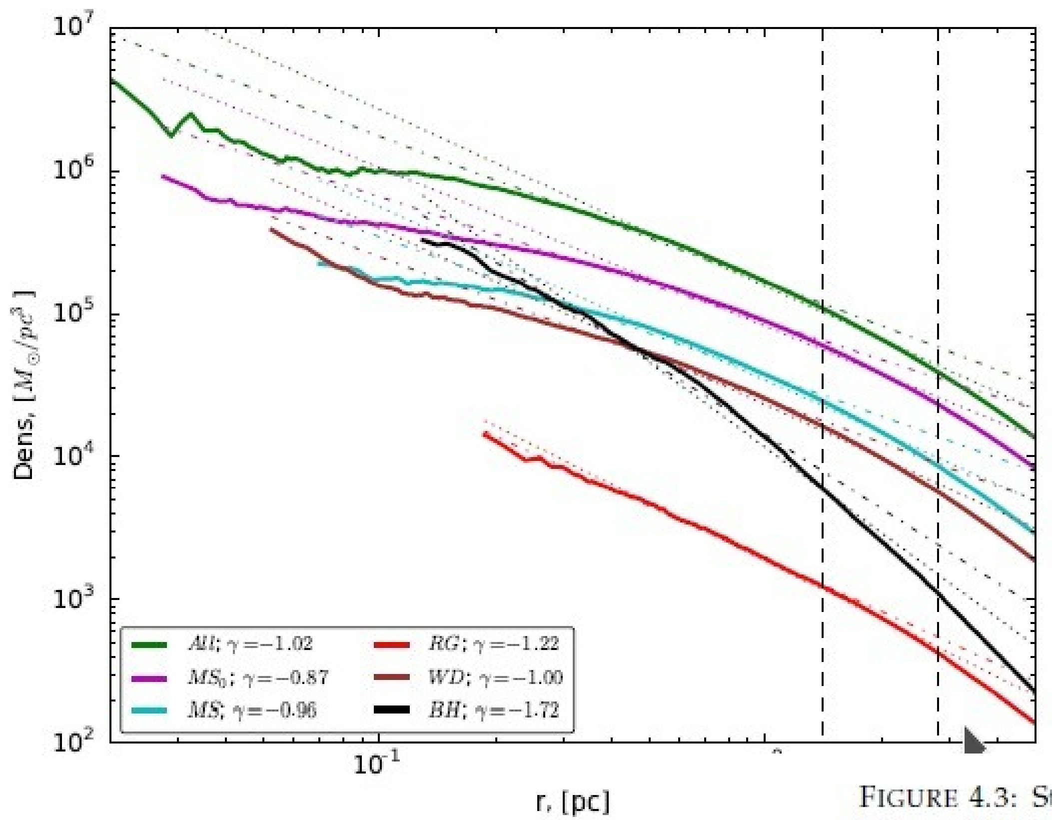


FIGURE 4.3: Stellar density profiles at t = 5 Gyr for different stellar types. Thick solid lines correspond to: All - all stars, $MS_{low}$ - low mass main sequence stars, MS - main sequence, RG - red giants, WD - white dwarfs, BH - black holes. Corresponding power-law slopes fitted inside the initial and final influence radii of the SMBH are shown as dash-dotted and dotted lines of the same colour. The dashed vertical lines denote the initial influence radius ($r = 1.4pc$) and the influence radius at $t = 5$Gyr ($r \sim 2.8pc$) of the SMBH. The power-law indices fitted inside $r = 1.4pc$ are shown in the legend.

**Initial Data:**

1 million stars

10% fixed SMBH mass

Zero age pop, 0.8 – 100

Spherical

Density Profiles of stars and *-mass Black Holes in the Galactic Center after 5 Gyr

**Extremely simple "accretion radius" For ALL objects.**

Panamarev, Just, Spurzem, et al. 2019

Panamarev, …, Just, Spurzem, 2018, MNRAS

# Tidal Disruption of a star by a SMBH

**Standard Picture**

Rees (1988)

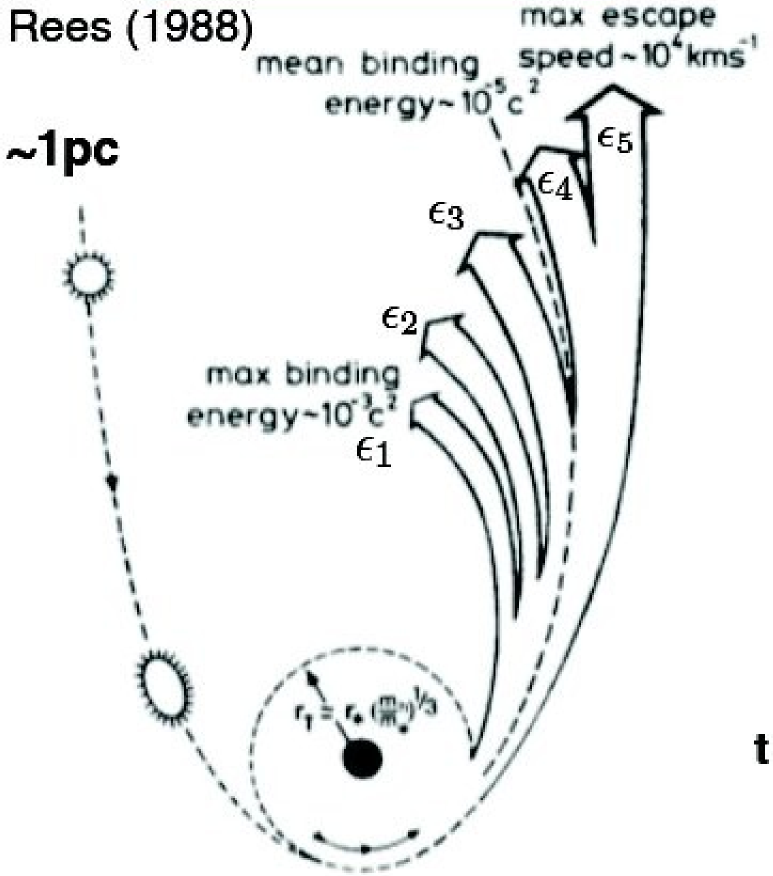


Tidal disruption radius
(Tidal force=self-gravity force):

$$r_t = \left(\frac{M_{BH}}{m_*}\right)^{1/3} r_*$$

**Δε: Spread in debris energy by tidal force**

$$\Delta\epsilon = \frac{GM_{BH}}{r_t}\frac{r_*}{r_t}$$

**ε: Debris specific energy**

| | |
|---|---|
| if ε>=0 | Stellar debris flies away from the black hole |
| if ε< 0 | Stellar debris is bounded by the black hole's gravity and falls back to black hole |

**t: Fallback time for most tightly bound debris**

$$t_{fall} \sim 0.1\,\mathrm{yr}\left(\frac{r_*}{R_\odot}\right)^{3/2}\left(\frac{m_*}{M_\odot}\right)^{-1}\left(\frac{M_{BH}}{10^6 M_\odot}\right)^{1/2}$$

**What is the rate of mass fallback?**

Slide by Kimitake Hayasaki

# Mass fallback rate I.

$$\frac{dM}{dt} = \boxed{\frac{dM(\epsilon)}{d\epsilon}} \left| \frac{d\epsilon}{dt} \right| \quad (\epsilon < 0)$$

Specific energy: $\epsilon \approx -\frac{GM_{\rm BH}}{2a}$

Its time derivative:

$$\frac{d\epsilon}{dt} = -\frac{1}{3}(2\pi G M_{\rm BH})^{2/3} t^{-5/3}$$

(by using Keplerian third law)

$$\frac{dM}{dt} \propto t^{-5/3}$$

**Rees's conjecture (1988)**

Differential mass-energy distribution of stellar debris

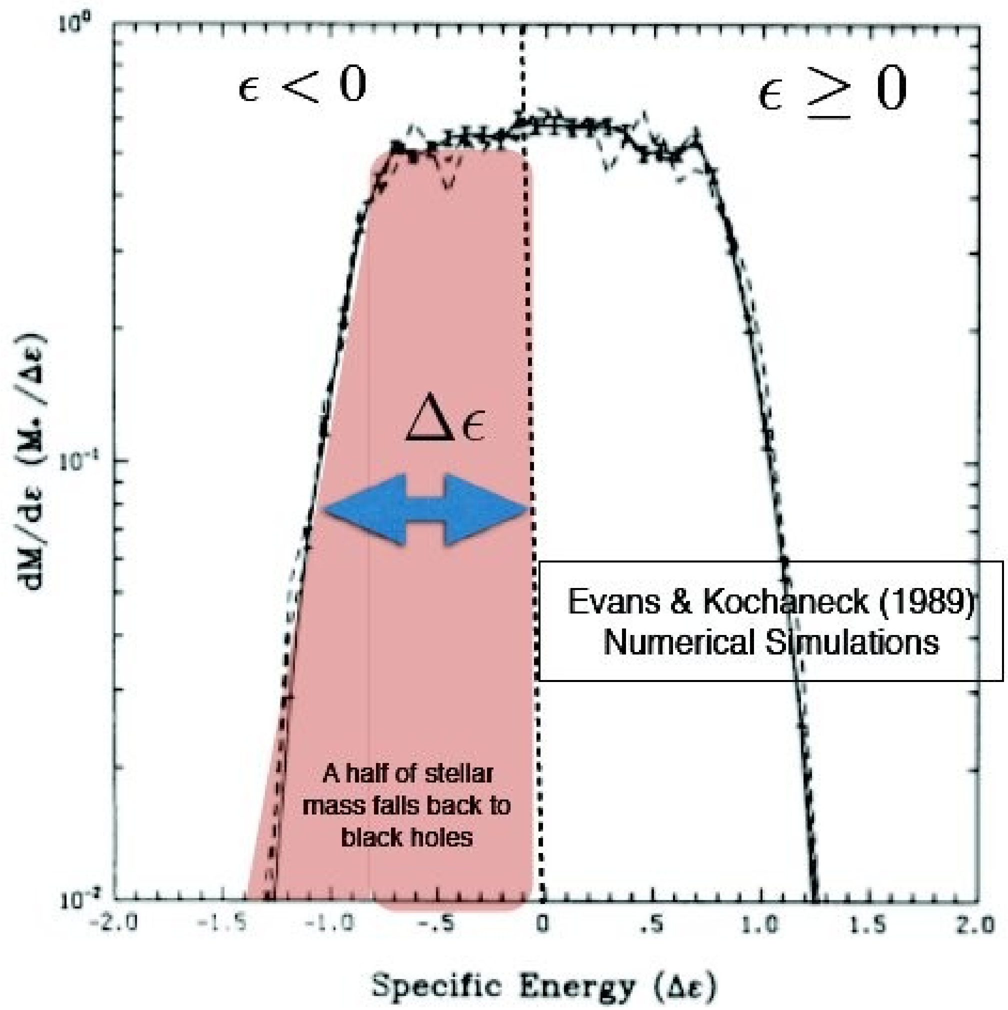


Slide by Kimitake Hayasaki

# Tidal Disruption — an Efficient Tool

- Disrupted stars can "light up" the dormant SMBH
- Special light curves in supermassive black hole binary (SMBHB) systems:
  *Liu et al. 2009, 2014, Ricarte et al. 2016, Coughlin et al. 2017*
- Different fallback rate (light curve?) for different orbits:
  - The fallback rate for eccentric (ECC) parabolic (PARA) and hyperbolic (HYP) are significantly different. In the extreme cases, all (ALLFB) / none (NOFB) debris could fallback:
    *Hayasaki et al. 2013, 2018, Park & Hayasaki 2020*
  - Most of disrupted stars in galaxies with single SMBHs are close to parabolic orbits:
    *Zhong et al. in prep.*
  - *Different for SMBHBs ?*


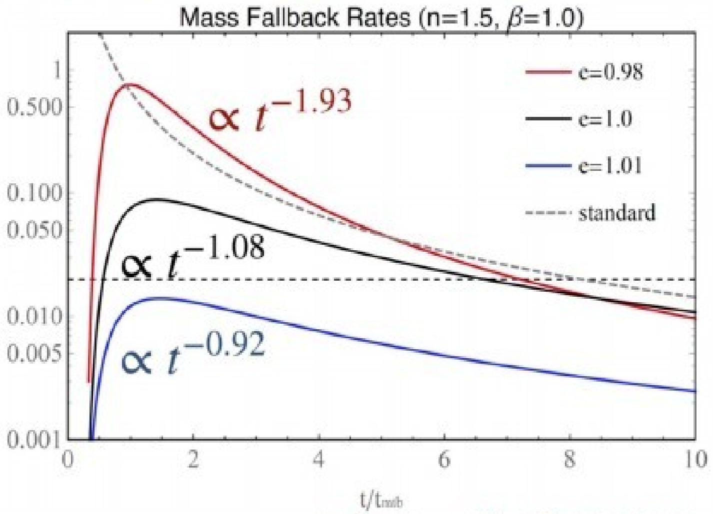


Park & Hayasaki, arXiv:2001.04548

Slide by Shuo Li

# Improvement 1:
# Partial and Full Tidal Disruption Events in Nuclear Star Cluster Simulations

From: Zhong, Li, Berczik, Spurzem, 2022, ApJ

THE ASTROPHYSICAL JOURNAL, 933:96 (13pp), 2022 July 1 Zhong et al.

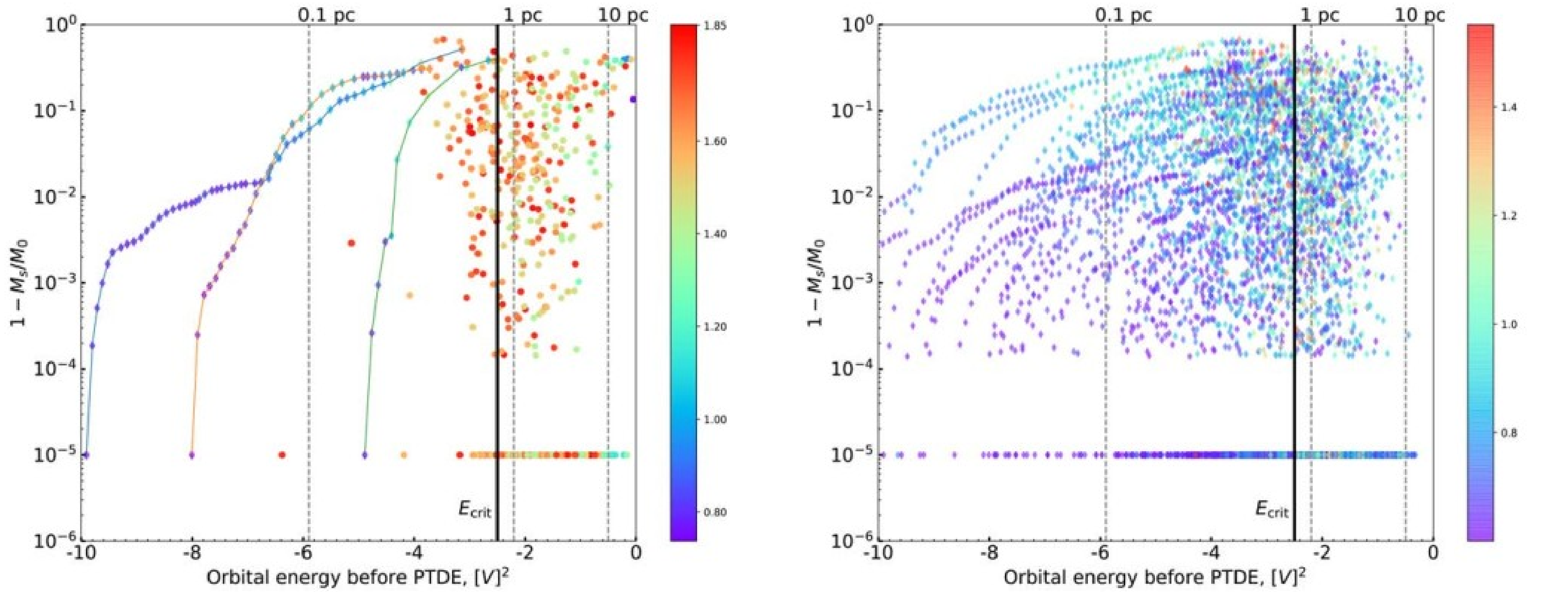


**Figure 4.** Distribution of stars that produce PTDEs in the parameter space spanned by the mass ($m_s$) and specific orbital energy ($E_{tot}$) of the stars. For every PTDE, the values of $m_s$ and $E_{tot}$ are measured at the moment immediately before the onset of the event. Colors indicate the penetration factor $\beta$. The vertical solid line marks the position of the critical energy, and the corresponding physical radius is roughly 0.7 pc. For clarity, the vertical axis shows the quantity $1 - m_s/m_0$, where $m_0 = 1/N\,[M]$ is the initial mass of the star, and is set to log scale. However, with this configuration, the PTDEs produced by the normal stars are not visible in the figure because $1 - m_s/m_0 = 0$. We have artificially reset the value of $1 - m_s/m_0$ to $10^{-5}$ for the PTDEs produced by normal stars. The left panel shows the PTDEs after which the leftover stars are ejected, while the right panel shows the PTDEs after which the leftover stars are retained in the star cluster. In the left panel, we also plot the historical PTDEs (diamonds connected by lines) for three individual stars. This figure is generated from the data of one realization of the fiducial model.

## More PTDE than FTDE – orbits diverse!

1) Introduction, History, Theory

2) Star Cluster Dynamics with
Black Holes and Gravitational Waves

3) Nuclear Star Clusters

**4) People, Code(s) and Hardware**

5) Summary and References

# Code(s)

Nbody6++GPU

# Nbody6++GPU

https://github.com/nbody6ppgpu (Spurzem & Kamlah 2023, LRCA)

The Hermite Scheme: 4th Order on two time points

$$\vec{a}_0 = \sum_j G m_j \frac{\vec{R}_j}{R_j^3} \quad ; \quad \dot{\vec{a}}_0 = \sum_j G m_j \left[ \frac{\vec{V}_j}{R_j^3} - \frac{3(\vec{V}_j \cdot \vec{R}_j)\vec{R}_j}{R_j^5} \right] ,$$

$$\vec{x}_p(t) = \frac{1}{6}(t - t_0)^3 \dot{\vec{a}}_0 + \frac{1}{2}(t - t_0)^2 \vec{a}_0 + (t - t_0)\vec{v} + \vec{x} ,$$
$$\vec{v}_p(t) = \frac{1}{2}(t - t_0)^2 \dot{\vec{a}}_0 + (t - t_0)\vec{a}_0 + \vec{v} ,$$

Repeat Step 1 at $t_1$ using predicted x,v → $a_1$, å$_1$

# Nbody6++GPU

$$\frac{1}{2}\vec{a}^{(2)} = -3\frac{\vec{a}_0 - \vec{a}_1}{(t-t_0)^2} - \frac{2\dot{\vec{a}}_0 + \dot{\vec{a}}_1}{(t-t_0)}$$

$$\frac{1}{6}\vec{a}^{(3)} = 2\frac{\vec{a}_0 - \vec{a}_1}{(t-t_0)^3} - \frac{\dot{\vec{a}}_0 + \dot{\vec{a}}_1}{(t-t_0)^2} \ ,$$

The Hermite Step

Get Higher Derivatives

$$\vec{x}(t) = \vec{x}_p(t) + \frac{1}{24}(t-t_0)^4\vec{a}_0^{(2)} + \frac{1}{120}(t-t_0)^5\vec{a}^{(3)} \ ,$$

$$\vec{v}(t) = \vec{v}_p(t) + \frac{1}{6}(t-t_0)^3\vec{a}_0^{(2)} + \frac{1}{24}(t-t_0)^4\vec{a}_0^{(3)} \ .$$

The Corrector Step – this is not time symmetric!

(but can be made so by iteration if desirable)

# Nbody6++GPU

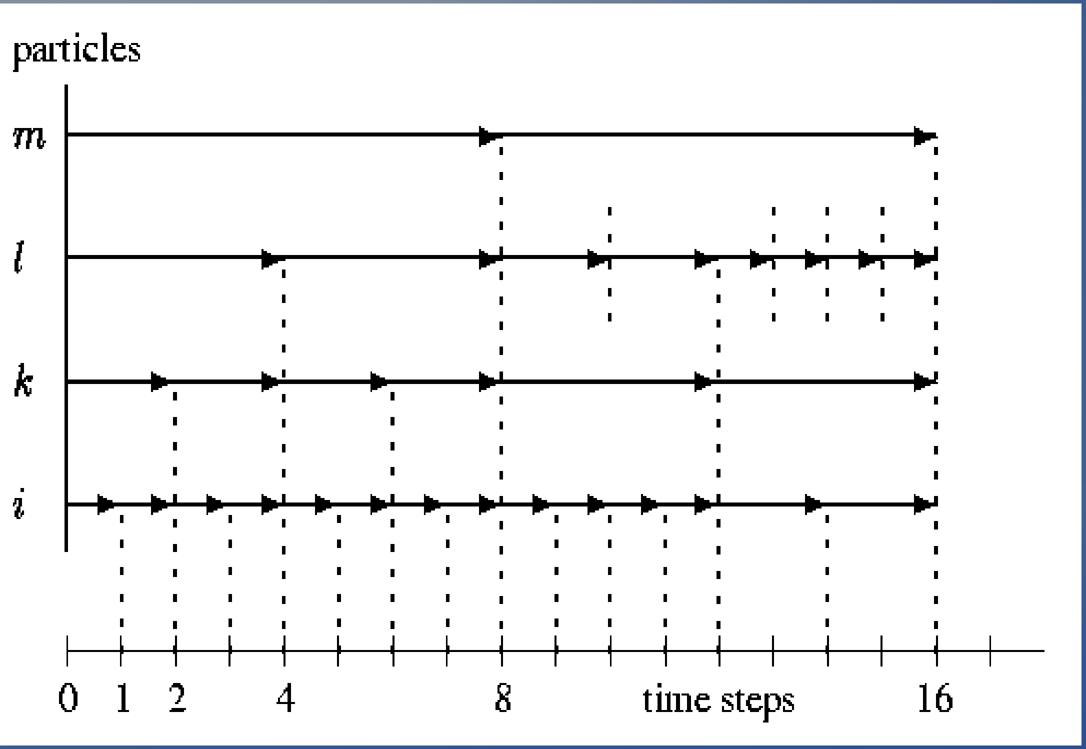


Hierarchical Block Time Steps

*S.J.Aarseth, S. Mikkola,*

*J. Hurley, R. Spurzem,*

*L. Wang, … (ca. 20.000 lines):*

- Hierarchical Block Time Steps
- Ahmad-Cohen Scheme
- Regularisations
- 4th order Hermite scheme

- NBODY6 (Aarseth 1999)
- NBODY6++ (Spurzem 1999) MPI
- NBODY6++GPU (Wang, Spurzem, Aarseth et al. 2015)

$$\Delta t = \sqrt{\eta \frac{|\vec{a}||\vec{a}^{(2)}| + |\dot{\vec{a}}|^2}{|\dot{\vec{a}}||\vec{a}^{(3)}| + |\vec{a}^{(2)}|^2}} \, .$$

# NBODY1 – NBODY7: “The Growth of an Industry” (Aarseth 1999)

| | ITS | ACS | KS | HITS | PN | AR | CC | MPI | GPU |
|---|---|---|---|---|---|---|---|---|---|
| NBODY1 | ✓ | | | | | | | | |
| NBODY2 | | ✓ | | ✓ | | | | | |
| NBODY3 | ✓ | | ✓ | | | | | | |
| NBODY4 | | | ✓ | ✓ | | | | | |
| NBODY5 | ✓ | ✓ | ✓ | | | | | | |
| NBODY6 | | ✓ | ✓ | ✓ | | | | | |
| NBODY6GPU | | ✓ | ✓ | ✓ | | | | ✓ | |
| NBODY6++ | | ✓ | ✓ | ✓ | | | ✓ | | |
| NBODY6++GPU | | ✓ | ✓ | ✓ | ✓ | | ✓ | ✓ | ✓ |
| NBODY7 | | ✓ | ✓ | ✓ | ✓ | ✓ | | | ✓ |

ITS: Individual time–steps [107]
ACS: Ahmad-Cohen neighbour scheme [109]
KS: KS–regularization of few-body subsystems [104]
HITS: Hermite scheme integration method combined with hierarchical block time-steps [111]
PN: Post-Newtonian [150, 125, 151]
AR: Algorithmic regularization [125]
CC: Classical chain regularization [114]
MPI: Message Passing Interface, multi-node multi-CPU parallelization [139]
GPU: use of GPU acceleration [138] (if also MPI: multi-node many GPU [144])

Berczik, Spurzem, et al., LNCS 2013; Table from: Spurzem, Kamlah 2023, LRCA

NBODY6++GPU: https://github.com/nbody6ppgpu/

Part of https://www.punch4nfdi.de/ PUNCH4NFDI Consortium w. Jülich

**Table 5.1:** Table showing important algorithmic, hardware and software development stepping stones in the development of direct *N*-body codes. The table is adapted from Aarseth (1999a), corrected in some places, but expanded to more recent developments.

| Year | Keyword | Reference |
|---|---|---|
| 1961 ...... | Force polynomial | (Aarseth, 1963) |
| | Individual time steps | (Aarseth, 1963) |
| | Gravitaitonal softening | (Aarseth, 1963) |
| 1966 ...... | Spherical harmonics | (Aarseth, 1967) |
| 1969 ....... | Two-body regularization | (Kustaanheimo & Stiefel, 1965) |
| 1972 ...... | Three-body regularization | (Aarseth & Zare, 1974) |
| 1973 ....... | Global regularization | (Heggie, 1974) |
| | Neighbor scheme | (Ahmad & Cohen, 1973) |
| 1978 ....... | Co-moving coordinates | (Aarseth, 1979) |
| 1979 ...... | Regularized AC | (Aarseth, 1985) |
| 1980 ....... | Planetary formation | (Lecar & Aarseth, 1986) |
| 1986 ....... | Hierarchical block-time steps | (McMillan, 1986) |
| 1989 ....... | Chain regularization | (Mikkola & Aarseth, 1990) |
| 1990 ....... | Particle in box scheme | (Aarseth, Lin, & Palmer, 1993) |
| 1991 ...... | Collisional tree code | (McMillan & Aarseth, 1993) |
| 1992 ....... | Chain *N*-body interface | (Aarseth, 1994) |
| 1993 ...... | Hermite integration | (Makino, 1991) |
| 1995 ....... | Synthetic stellar evolution | (Tout et al., 1997) |
| | Tidal circularization | (Mardling, 1995a, 1995b) |
| | Slow chain regularization | (Mikkola & Aarseth, 1998) |
| 1996 ...... | Hierarchical stability | (Mardling & Aarseth, 1999) |
| 1998 ....... | Evolution of hierarchies | (Mardling & Aarseth, 1999) |
| | Stumpff KS method | (Mikkola & Aarseth, 1998) |
| 1999 ...... | HARP-6 procedures | (Aarseth, 1999a) |
| | Sympletic integrators | (Mikkola & Tanikawa, 1999b, 1999a) |
| | NBODY6++ SPMD / MPI acceleration | (Spurzem, 1999) |
| 2000 ...... | Single stellar evolution - SSE | (Hurley, Pols, & Tout, 2000) |
| 2002 ...... | Binary stellar evolution - BSE | (Hurley, Tout, & Pols, 2002) |
| 2003 ...... | GRAPE-6 procedures | (Makino et al., 2003) |
| 2006 ...... | 2.5PN in NBODY5 | (Kupi, Amaro-Seoane, & Spurzem, 2006) |
| 2007 ...... | direct *N*-body GPU acceleration | (Portegies Zwart, Belleman, & Geldof, 2007) |
| 2008 ...... | AR with Post-Newtonian terms | (Mikkola & Merritt, 2008) |
| 2010 ...... | Updated AR for few-body problems | (Hellström & Mikkola, 2010) |
| 2012 ...... | NBODY codes GPU acceleration | (Nitadori & Aarseth, 2012) |
| 2013 ...... | MPI acceleration on GPU clusters / PHIGPU | (Berczik et al., 2013) |
| | 3.5PN in NBODY6 | (Brem, Amaro-Seoane, & Spurzem, 2013) |
| 2015 ...... | SSE/AVX acceleration on GPU clusters | (Wang et al., 2015) |
| 2017 ...... | Sympletic integrators (FSI) | (Dehnen & Hernandez, 2017) |
| 2020 ...... | P³T with SDAR in PETAR | (Wang, Nitadori, & Makino, 2020a; Wang et al., 2020a) |
| 2021 ...... | Minimum spanning tree MSTAR/BIFROST | (Rantala, Naab, & Springel, 2021) |

From: Spurzem, Kamlah, Living Review Computational Astrophysics Vol. 9, pp. 3-109 2023

# Code (Stellar Evolution)

## SSE  BSE and Updates

Single Stellar Evolution
Binary Stellar Evolution
(Multiple Stellar  Evolution, MSE, Future)

# Most NBODY Codes ...

Hurley,
Ph.D. thesis

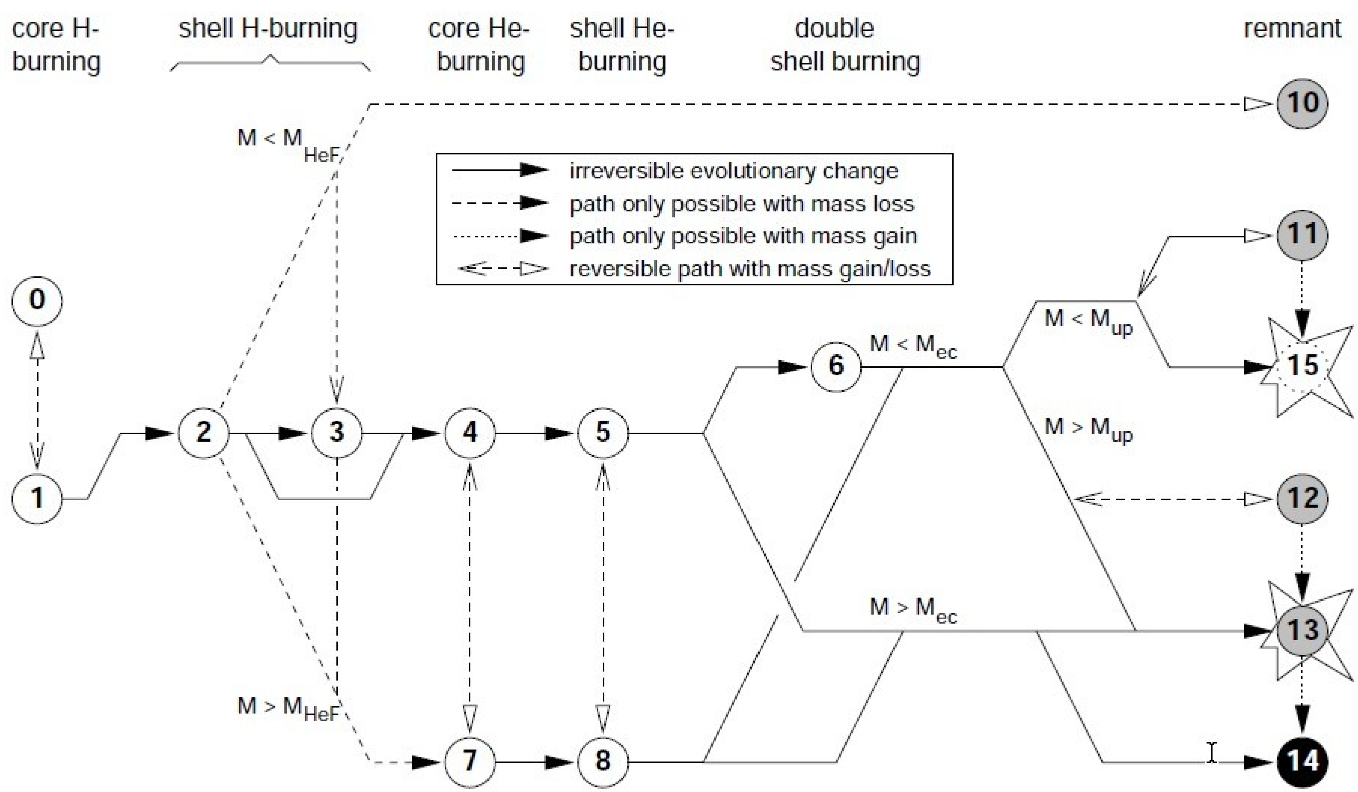


0 = main sequence $M < 0.7\,M_\odot$
1 = main sequence $M > 0.7\,M_\odot$
2 = Hertzsprung gap / subgiant
3 = first-ascent red giant
4 = horizontal branch / helium-burning giant
5 = early asymptotic giant / red supergiant
6 = thermally pulsating asymptotic giant

7 = naked helium main sequence
8 = naked helium (sub) giant
10 = helium white dwarf
11 = carbon/oxygen white dwarf

12 = oxygen/neon white dwarf
13 = neutron star
14 = black hole
15 = no stellar remnant

# Parameterized stellar evolution tracks (IFMR for neutron stars and white dwarfs)

(SSE++/BSE++ from Kamlah et al. 2022 and Spurzem & Kamlah, Living Reviews Comp. Astroph. 2023)

- updated metallicity dependent core-collapse SNe, their remnant masses and fallback (Fryer et al. 2012; Banerjee et al. 2020),
- updated electron-capture supernovae (ECSNe), accretion-induced collapse (AIC) and merger-induced collapse (MIC) remnant masses and natal kicks (Nomoto 1984, 1987; Nomoto & Kondo 1991; Saio & Nomoto 1985, 2004; Kiel et al. 2008; Gessner & Janka 2018)
- (P)PISNe remnant masses (Belczynski et al. 2010, 2016; Woosley 2017),
- updated fallback-scaled natal kicks for NSs and BHs (Fuller et al. 2003; Scheck et al. 2004; Fryer 2004; Fryer & Kusenko 2006; Meakin & Arnett 2006, 2007; Fryer & Young 2007; Scheck et al. 2008; Fryer et al. 2012; Banerjee et al. 2020),
- and BH natal spins (see also Belczynski et al. (2020); Belczynski & Banerjee (2020)) from
  - `Geneva` model (Eggenberger et al. 2008; Ekström et al. 2012; Banerjee et al. 2020; Banerjee 2021b),
  - `MESA` model (Spruit 2002; Paxton et al. 2011, 2015; Banerjee et al. 2020; Banerjee 2021b),
  - and the `Fuller` model (Fuller & Ma 2019; Fuller et al. 2019; Banerjee et al. 2020; Banerjee 2021b).

ECSN = electron capture Supernova

AIC = accretion induced collapse

MIC = merger induced Collapse

PISN = pair instability Supernova

PPISN = pulsating PISN

NS = neutron star

BH = black hole

MESA = recent stellar evolution model

# Parameterized stellar evolution tracks
# (IFMR for neutron stars and white dwarfs)

(SSE++/BSE++ from Kamlah et al. 2022)

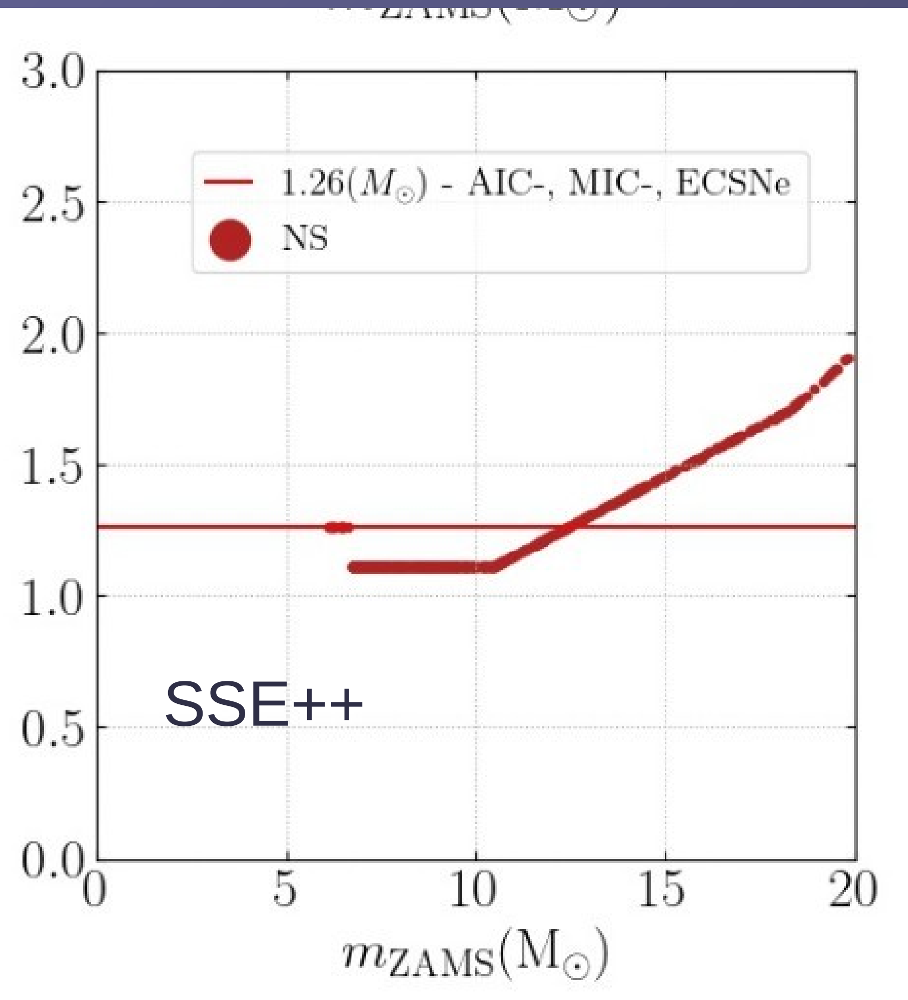


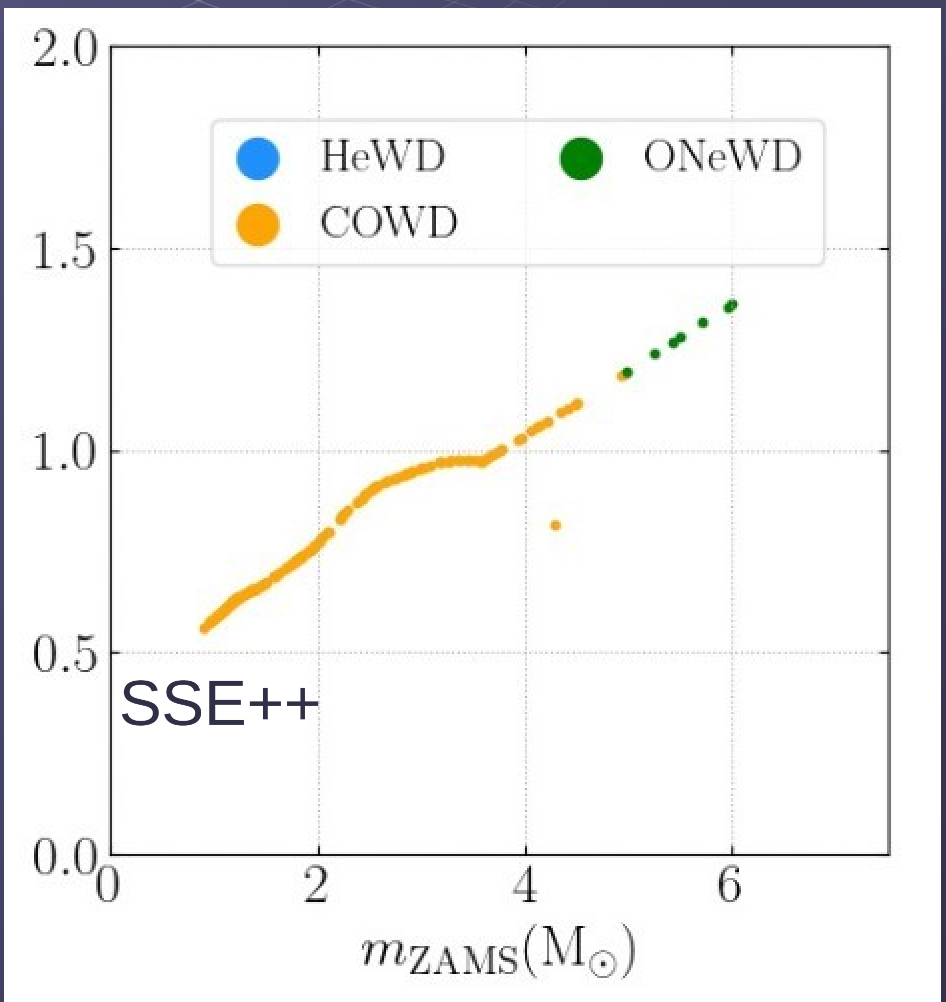

# Codes

Parallelization
Supercomputing
GPU Computing

# Our own φGRAPE/GPU N-body code

~N

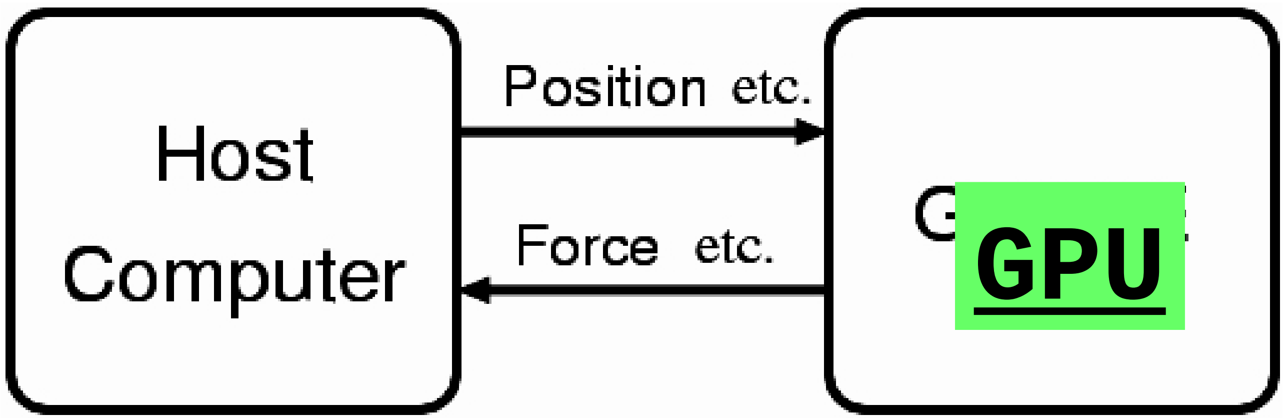


~N^2

$$\vec{a}_i = \sum_{j=1; j \neq i}^{N} \vec{f}_{ij} \qquad \vec{f}_{ij} = -\frac{G \cdot m_j}{\left(r_{ij}^2 + \varepsilon^2\right)^{3/2}} \vec{r}_{ij}$$

Slide: Peter Berczik

## *NBODY6++GPU*

https://github.com/nbody6ppgpu/Nbody6PPGPU-beijing

Picture by
Long Wang

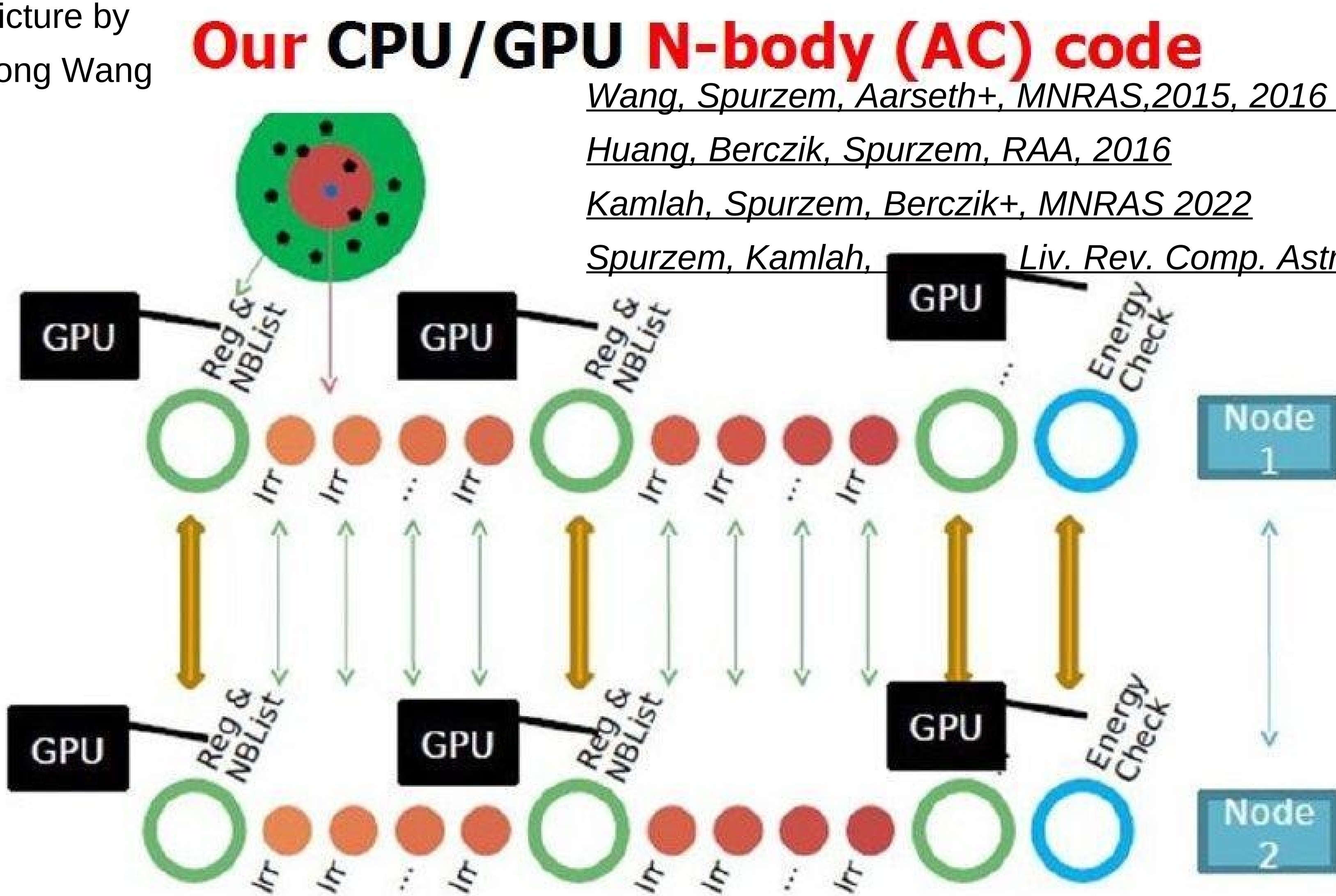


*Wang, Spurzem, Aarseth+, MNRAS,2015, 2016*

*Huang, Berczik, Spurzem, RAA, 2016*

*Kamlah, Spurzem, Berczik+, MNRAS 2022*

*Spurzem, Kamlah, Liv. Rev. Comp. Astroph. 2023*

*Huang, Berczik, Spurzem, RAA, 2016*

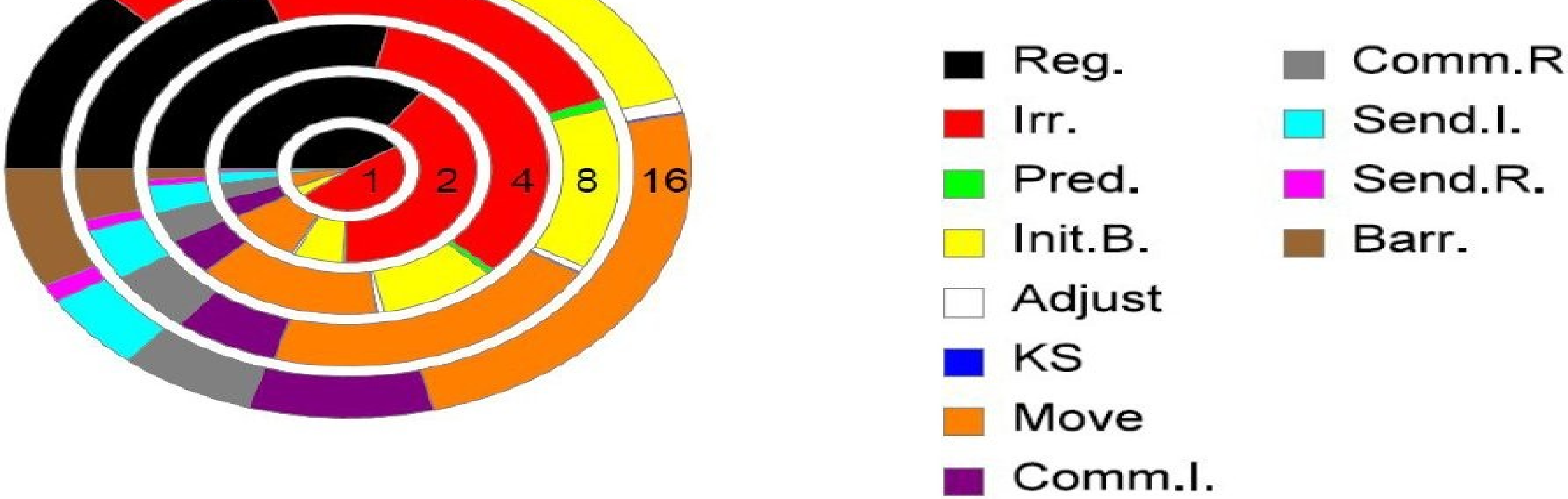


**Table 1** Main components of NBODY6++

| Description | Timing variable | Expected scaling $N$ | Expected scaling $N_p$ | Fitting value [sec] |
|---|---|---|---|---|
| Regular force computation | $T_{\rm reg}$ | $\mathcal{O}(N_{\rm reg} \cdot N)$ | $\mathcal{O}(N_p^{-1})$ | $(2.2 \cdot 10^{-9} \cdot N^{2.11} + 10.43) \cdot N_p^{-1}$ |
| Irregular force computation | $T_{\rm irr}$ | $\mathcal{O}(N_{\rm irr} \cdot \langle N_{nb} \rangle)$ | $\mathcal{O}(N_p^{-1})$ | $(3.9 \cdot 10^{-7} \cdot N^{1.76} - 16.47) \cdot N_p^{-1}$ |
| Prediction | $T_{\rm pre}$ | $\mathcal{O}(N^{kn_p})$ | $\mathcal{O}(N_p^{-kp_p})$ | $(1.2 \cdot 10^{-6} \cdot N^{1.51} - 3.58) \cdot N_p^{-0.5}$ |
| Data moving | $T_{\rm mov}$ | $\mathcal{O}(N^{kn_{m1}})$ | $\mathcal{O}(1)$ | $2.5 \cdot 10^{-6} \cdot N^{1.29} - 0.28$ |
| MPI communication (regular) | $T_{\rm mcr}$ | $\mathcal{O}(N^{kn_{cr}})$ | $\mathcal{O}(kp_{cr} \cdot \frac{N_p-1}{N_p})$ | $(3.3 \cdot 10^{-6} \cdot N^{1.18} + 0.12)(1.5 \cdot \frac{N_p-1}{N_p})$ |
| MPI communication (irregular) | $T_{\rm mci}$ | $\mathcal{O}(N^{kn_{ci}})$ | $\mathcal{O}(kp_{ci} \cdot \frac{N_p-1}{N_p})$ | $(3.6 \cdot 10^{-7} \cdot N^{1.40} + 0.56)(1.5 \cdot \frac{N_p-1}{N_p})$ |
| Synchronization | $T_{\rm syn}$ | $\mathcal{O}(N^{kn_s})$ | $\mathcal{O}(N_p^{kp_s})$ | $(4.1 \cdot 10^{-8} \cdot N^{1.34} + 0.07) \cdot N_p$ |
| Sequential parts on host | $T_{\rm host}$ | $\mathcal{O}(N^{kn_h})$ | $\mathcal{O}(1)$ | $4.4 \cdot 10^{-7} \cdot N^{1.49} + 1.23$ |

# NBODY6++GPU with up to 16M particles

## (Benchmarks on raven at MPCDF)

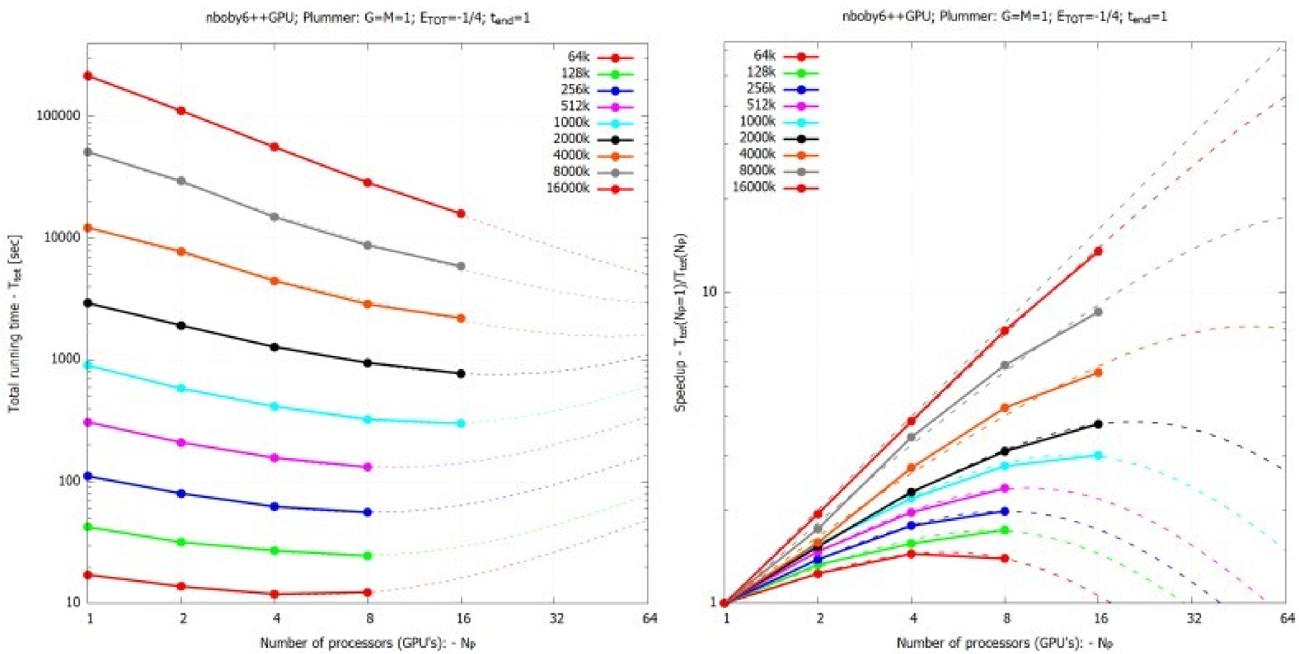


Figure 6: Benchmark results and extrapolated scaling for NBODY6++GPU, initial Plummer model, on the raven cluster at MPCDF, see main text. **Left:** Total time for one NBODY model unit in secs; **Right:** Speed-Up compared to using one GPU only. In both cases different curves for particle numbers from 64k to 16m. Ideal Speedup is the diagonal dashed lines, other dashed lines extrapolations from the timing model.

# PeTar: a high-performance $N$-body code for modeling massive collisional stellar systems

Long Wang,[1,2★] Masaki Iwasawa,[2,3] Keigo Nitadori[2] and Junichiro Makino[2,4]
[1]Department of Astronomy, School of Science, The University of Tokyo, 7-3-1 Hongo, Bunkyo-ku, Tokyo, 113-0033, Japan
[2]RIKEN Center for Computational Science, 7-1-26 Minatojima-minami-machi, Chuo-ku, Kobe, Hyogo 650-0047, Japan
[3]National Institute of Technology, Matsue College, 14-4, Nishi-ikuma-cho, Matsue, Shimane 690-8518, Japan
[4]Graduate School of Science, Kobe University, 1-1 Roki Slide 50 ho, Nada-ku, Kobe, Hyogo 657-8501, Japan

Accepted XXX. Received YYY; in original form ZZZ

***New competition 1:***

***PeTar: MNRAS 2020***

**ABSTRACT**
The numerical simulations of massive collisional stellar systems, such as globular clusters (GCs), are very time-consuming. Until now, only a few realistic million-body simulations of GCs with a small fraction of binaries (5%) have been performed by using the NBODY6++GPU code. Such models took half a year computational time on a GPU based super-

# FROST: a momentum-conserving CUDA implementation of a hierarchical fourth-order forward symplectic integrator

Antti Rantala[1★], Thorsten Naab[1], Volker Springel[1]
[1]Max-Planck-Institut für Astrophysik, Karl-Schwarzschild-Str. 1, D-85748, Garching, Germany

***New competition 2:***

***FROST: MNRAS 2021***

Slide 50

Accepted XXX. Received YYY; in original form ZZZ

**ABSTRACT**
We present a novel hierarchical formulation of the fourth-order forward symplectic integrator and its numerical implementation in the GPU-accelerated direct-summation N-body code FROST. The new integrator is especially suitable for simulations with a large dynamical range due to its hierarchical nature. The strictly positive integrator sub-steps in a fourth-

# Supercomputers

# HARDWARE

...before von Neumann...

- Konrad Zuse (1910-1995) Berlin

**Invented freely programmable Computer**

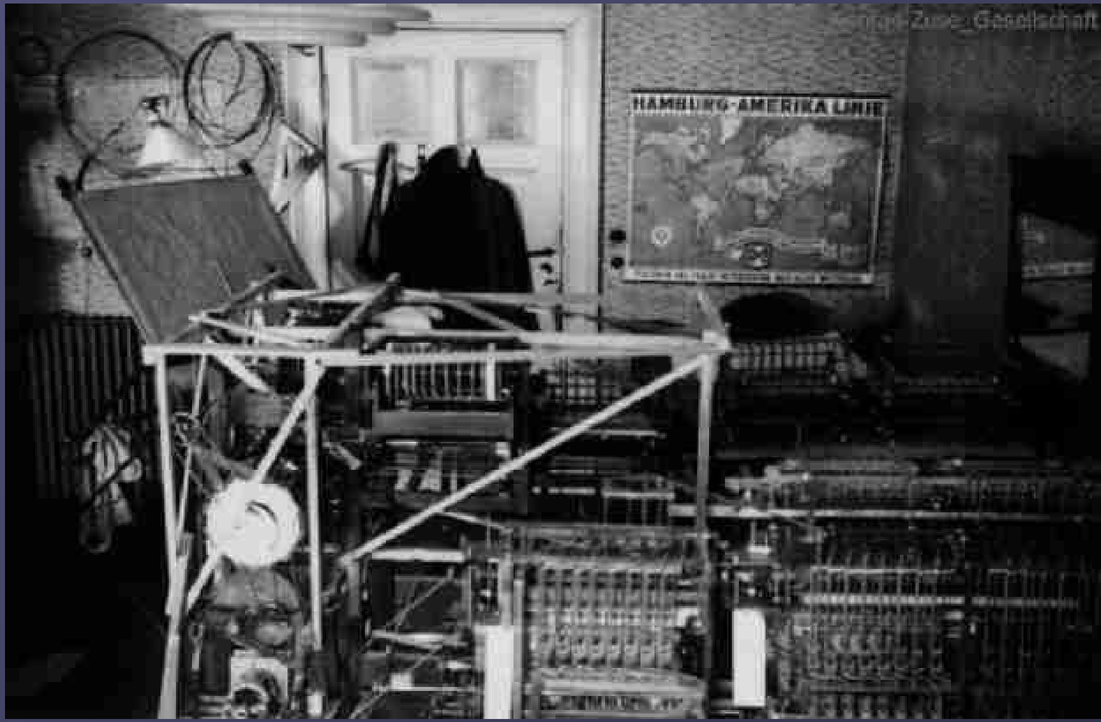


**Z1 in parental flat 1936**

# A special-purpose computer for gravitational many-body problems

Nature 1990

**Daiichiro Sugimoto*, Yoshihiro Chikada†, Junichiro Makino*, Tomoyoshi Ito*, Toshikazu Ebisuzaki* & Masayuki Umemura‡**

* Department of Earth Science and Astronomy, College of Arts and Sciences, University of Tokyo, 3-8-1 Komaba, Meguro-ku, Tokyo 153, Japan
† Nobeyama Radio Observatory, Minamimaki-mura, Minamisaku-gun, Nagano 384-13, Japan
‡ National Astronomical Observatory, Mitaka, Tokyo 181, Japan

A processor has been constructed using a 'pipeline' architecture to simulate many-body systems with long-range forces. It has a speed equivalent to 120 megaflops, and the architecture can be readily parallelized to make teraflop machines a feasible possibility. The machine can be adapted to study molecular dynamics, plasma dynamics and astrophysical hydrodynamics with only minor modifications.

(very-large-scale
puter is construc
lem is to devel
construction and
of physical syste
to these apparent
ted in the compu
GRAPE-1 achie
XMP/1 at a cos

**The pipeline a**

The *N*-body pro

## GRAPE-6 Gravity/Coulomb Part

- G6 Chip: 0.25$\mu$ 2MGate ASIC, 6 Pipelines
- at 90MHz, 31Gflops/chip
- 48Tflops full system (March 2002)
- Plan up to 72Tflops full system (in 2002)
- Installed in Cambridge, Marseille, Drexel, Amsterdam, New York (AMNH), Mitaka (NAO), Tokyo, etc..

Jun Makino
with GRAPE6 →
(2002)

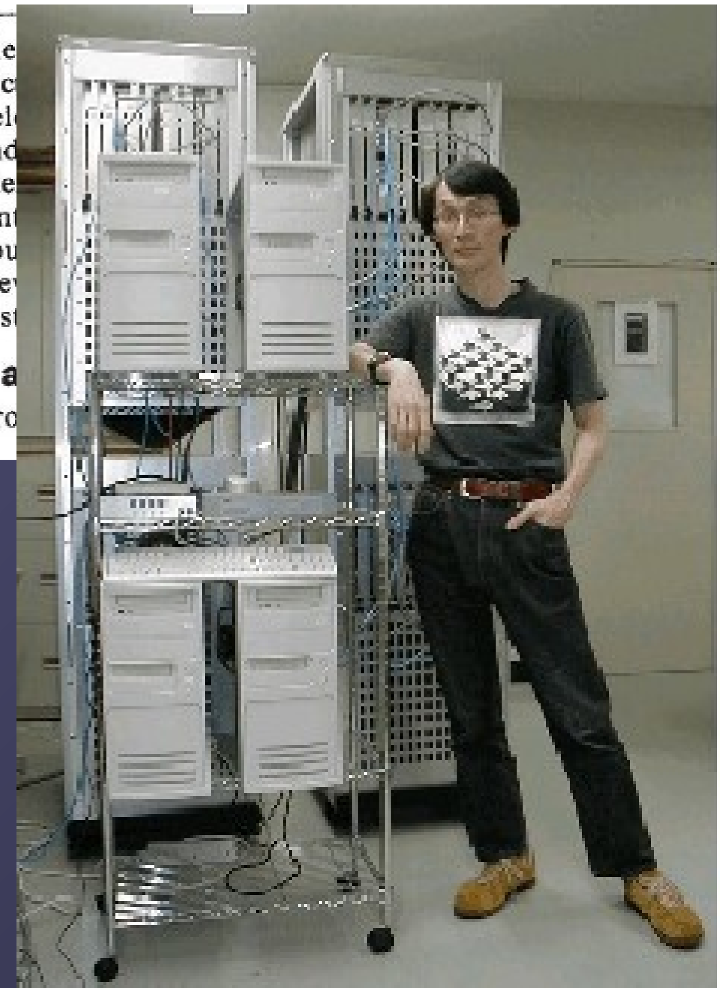

# NAOC laohu cluster

**64 Kepler K20**

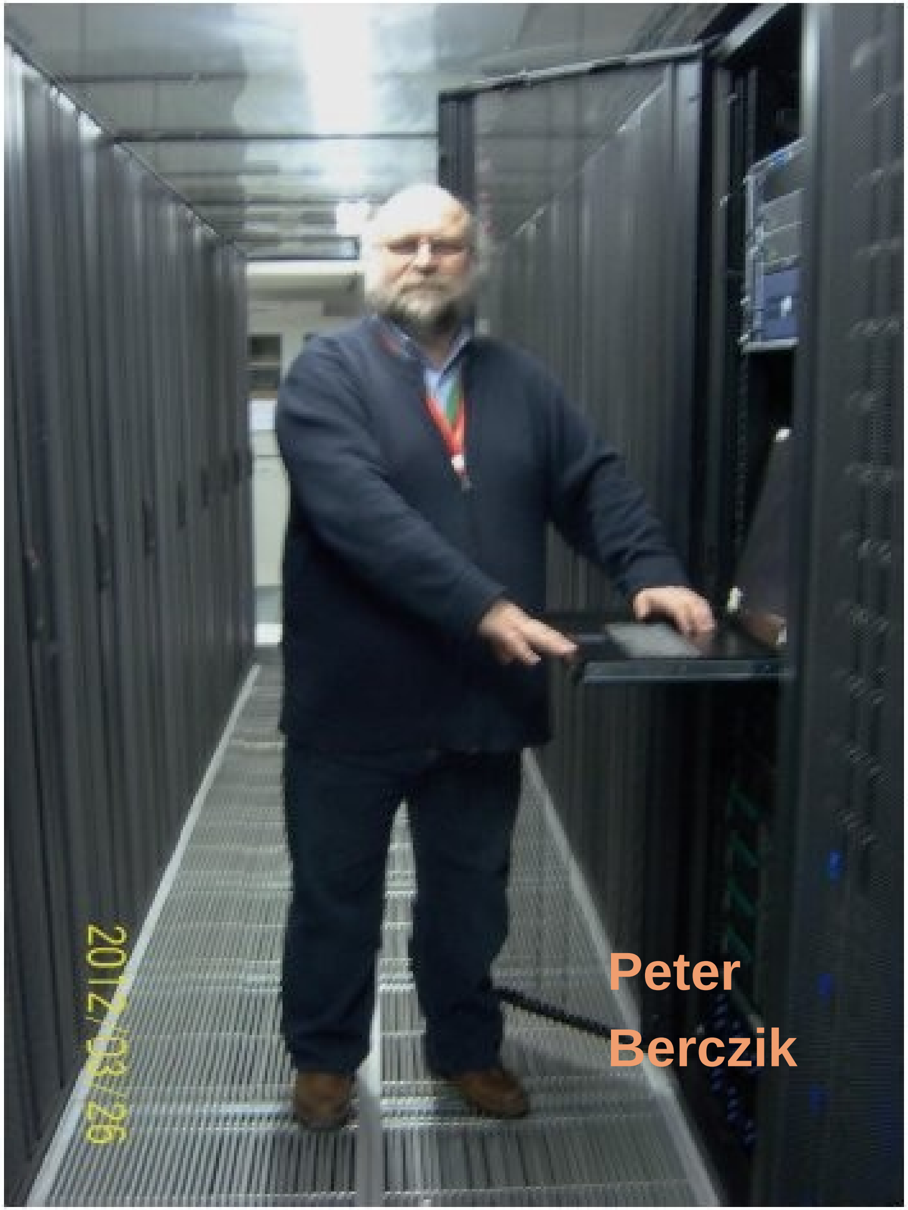


**Laohu: 2009/2015**
**(Kepler GPU)**
**100 Tflop/s 150k cores**

**New GPUs 5-6 times faster… (see below)**

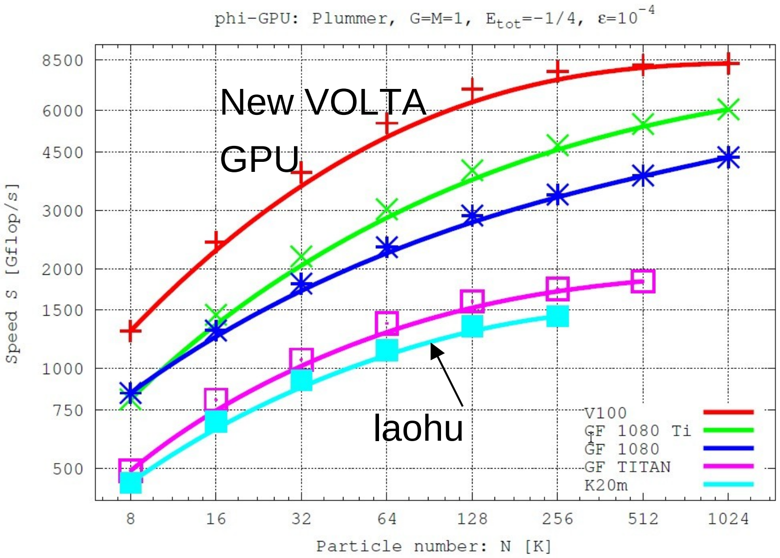

## *GPU Clusters used:*

**Kepler Cluster Heidelberg, Germany**

(12x Kepler GPU, each ~2400 GPU cores)

**Hansolo/Obiwan GPU Servers Beijing, China**

(4x GTX 2080 GPU, each ~4300 GPU cores)

**<u>JUWELS Booster GPU Partition (Ampere A100 GPU)</u>**

(936 x 4 Ampere A100 GPU, each ~7000 GPU cores)

**<u>Raven GPU Cluster of Max-Planck Computing and Data Facility</u>**

MPCDF Garching

**Peter Berczik, golowood Cluster Main Astron. Observatory Kiev, Ukraine**

**Heidelberg Germany**

Hansolo @ NAOC
Silk Road Project


**JUWELS Juelich GPU Cluster Germany**

JUWELS Booster 936 nodes (AMD CPU, 4x Ampere GPU)

~450.000 AMD cores, 25 million NVIDIA Ampere GPU cores

~ 70 Pflop/s SP ~ 44 Pflop/s DP

No. 12 in top500 list, No. 25 in green500 list

**Jülich Wizard for European Leadership Science**

LUMI

# Supercomputer, Kajaani, Finland


Using only

Hydroelectric

Power and its

Heat used for heating buildings.

No. 3 in top500

No. 7 in green500

2.2 million cores

10.000 AMD GPUs


EuroHPC and LUMI consortium:

Finland, Belgium, Czech Republic, Denmark, Estonia, Iceland, Norway, Poland, Sweden, and Switzerland.

# China New Computing Technology 2

Hygon CPU/DCU (Deep Computing Unit)
(~ AMD EPYC/AMD GPU HIP programming language

**V100的全面国产替代 ——海光DCU Z100L 面向人工智能的GPGPU加速卡**

mzzy
服务器厂家

**Details OUTDATED, just for illustration**

简单介绍一下海光的这款产品

DCU (Deep Computing Unit) Z100L 是一款面向人工智能、科学计算的高性能全功能GPGPU加速卡。

| 规格参数 | | Z100L及Z100L-LP | |
|---|---|---|---|
| 应用场景 | | 全精度支持 | AI优化 |
| 适配服务器 | | 2U/4U风冷服务器 | |
| 构架核心 | 计算核心 | 3840 | |
| | 频率 | 1319MHz | 1600MHz |
| 性能指标 | FP64 | 10.1TFlops | ——— |
| | FP32 | 10.1TFlops | 12.2TFlops |
| | FP16 | 20.2TFlops | 24.5TFlops |
| | INT8 | 40.5TFlops | 49.1TFlop |
| 存储规格 | 显存容量 | 32GB HBM2 | |
| | 显存带宽 | 1024 GB/s | |
| 接口类型 | PCIe 接口 | PCIe 4.0 x16 | |
| | GPU 互联 | xHMI互联 184GB/s | |
| 最大功耗 | TDP | 250W | 280W |
| 尺寸规格 | 尺寸 | 全高全长双宽 | |



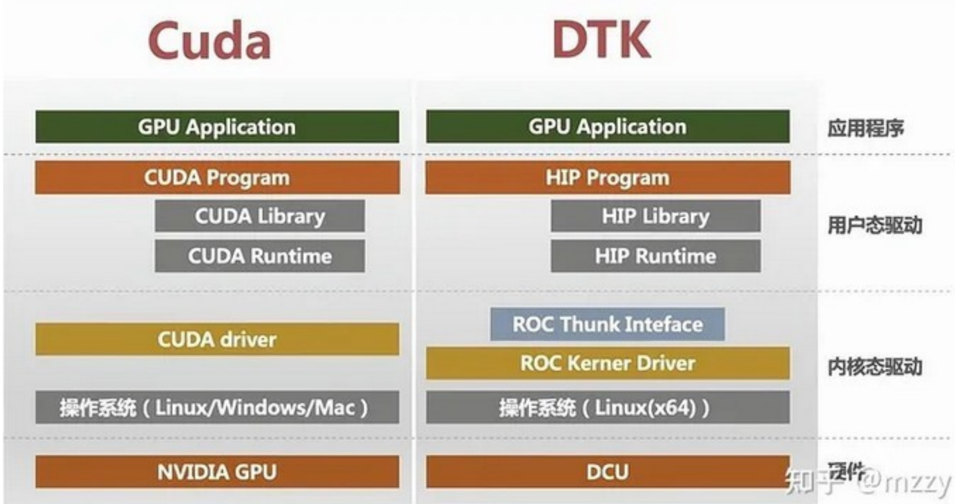


| CUDA数学库 | DTK数学库 | 数学库功能 |
|---|---|---|
| cudnn | miopen | 深度学习基础数学库 |
| cublas | rocblas/hipblas | 基础矩阵运算数学库 |
| nccl | rccl | 通信库 |

| | Juwels-Booster | Beijing DCU cluster ("东方"超算) |
|---|---|---|
| CPU | 48 core, AMD EPYC 7402 | 30 core, HYGON C86 7185 |
| GPU | 4 x NVIDIA A100 GPU | 4 x HYGON [redacted] DCU |
| #Node used | 1 | 1 |
| #MPI proc | 4 | 4 |
| Code version | CUDA (standard GitHub) | HIP |
| Time to run 1M body for 1nbody time | 810 seconds | 1605 seconds |

## ⟸ last week

Kai Wu preliminary results: 1st benchmarks of Nbody6++GPU on Chinese DCU

1) Introduction, History, Theory

2) Star Cluster Dynamics with
Black Holes and Gravitational Waves

3) Nuclear Star Clusters

4) People, Code(s) and Hardware

**<u>5) Summary and References</u>**

# Summary Message

***Massive Star Clusters:***

- Direct N-Body Simulations of star clusters give LIGO/Virgo Sources (are consistent with them, it does not mean all sources are from star clusters)
- Necessary Input: single/binary stellar evolution / relativistic (PN) dynamics
- Still very long computing time for few models (in spite of GPU, Lumi, …)

Monte Carlo Models (MOCCA, Warsaw, M. Giersz, CMC, Northwestern, F. Rasio) needed to get good sweep of parameter space, comparison with N-Body

***Nuclear Star Clusters:***

- Observable Tidal Disruption Events (TDE)
- Light Curves correspond to dynamics of TDE
- Future Work: relativistic inspirals
- Future Work: pulsars
- Future Work: star disk

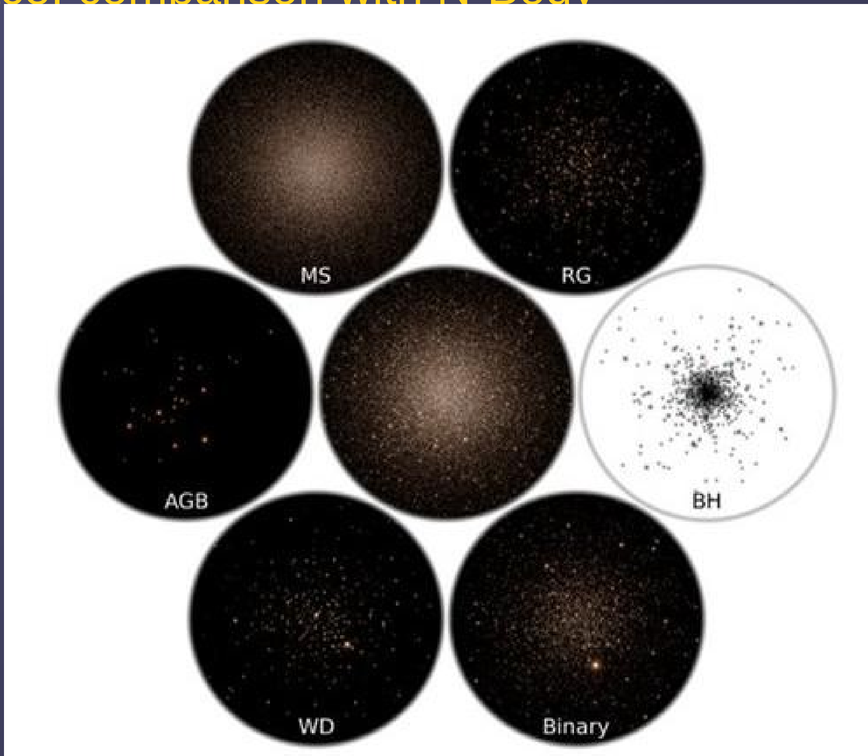


# The Future - DRAGON III 1m – 8m (16m?)

## Only few models, 6-12 months

Request for Comments, Feedback, Initial Conditions: Call will go out, or contact

spurzem@ari.uni-heidelberg.de spurzem@nao.cas.cn

- Globular Cluster (GC) Simulations: Init. Density, IMF, Binaries (wide?), Rotation, Populations, Tides, GC orbit, specific clusters, …
- Nuclear Star Cluster (NSC) Simulations: add TDE, EMRI, direct capture, partial TDE, partial accretion to SMBH.

# Team & Collaborators as below and further:

Francesco Flammini Dotti, Kai Wu, Li Shuo, Zhong Shiyan, Peter Berczik, Manuel Arca Sedda (GSSI), Thorsten Naab (MPA), Mirek Giersz (CAMK)
PhD students: Vahid Amiri, Marcelo Vergara, Philip Cho

ARI ITA LSW

## DRAGON simulations – globular and nuclear star clusters

- **DRAGON simulation: PhD thesis Long Wang, KIAA/PKU,** awarded for first realistic globular cluster simulation using NBODY6++GPU with one million stars and many binaries (Wang, Spurzem, Aarseth, et al., MNRAS 2016).
- **The Dragon-II simulations – Paper III. Compact binary mergers in clusters with up to 1 million stars: mass, spin, eccentricity, merger rate and pair instability supernovae rate** (Arca Sedda, M., Kamlah, A. W. H., Spurzem, R., et al.) arXiv e-prints arXiv:2307.04807, **Paper II:** MNRAS 525, 429 (2023), **Paper I:** arXiv e-prints arXiv:2307.04805

## NBODY6++GPU and more, current state:

- Spurzem, R., Kamlah A.W.H. **Direct N-body simulations, in Living Rev. in Comp. Astrophysics 9, id.3 (2023) (NBODY7 see also Banerjee, Sambaran papers)**

## Direct Nuclear Star Cluster Models with SMBH and TDE:

- **DRAGON simulation of the Galactic Center**, PhD thesis of Taras Panamarev, ARI/ZAH Univ. of Heidelberg (Panamarev, Just, Spurzem, Berczik, Wang, Arca Sedda, MNRAS 2019), simple TDE
- **Revisit the Rate of Tidal Disruption Events: The Role of the Partial Tidal Disruption Event** (Zhong, S., Li, S., Berczik, P., Spurzem, R.) 933, 96 (2022), TDE improved 1
- Marija Minzburg, Philip Cho: Master Thesises Heidelberg 2023, publication in progress, TDE improved 2 and 3.

## Some other papers and collaborators may be mentioned:

- Rizzuto, Naab, Spurzem et al. (2021, 2022) precursor of DRAGON II but no GW kicks, no TDE
- Li, Zhong, Berczik, Spurzem, Chen, Liu (MNRAS 2023 and earlier): merging nuclei with TDE